Long-Term Sleep Assessment by Unobtrusive Pressure Sensor Arrays

By

Sareh Soleimani

Thesis submitted

In partial fulfillment of the requirements

For the Master of Applied Science degree in Electrical and Computer Engineering

Ottawa-Carleton Institute for Electrical and Computer Engineering

School of Electrical Engineering and Computer Science

Faculty of Engineering

University of Ottawa

Abstract

Due to a globally aging population, there is a growing demand for smart home technology which can serve to monitor the health and safety of adults. Therefore, sleep monitoring has emerged as a crucial tool to improve the health and autonomy of adults. While polysomnography (PSG) is an effective and accurate tool for sleep monitoring, it is obtrusive as the user must wear the instruments during the experiment. Therefore, there has been a growing interest in deploying unobtrusive sleep monitoring devices, specifically for long-term patient monitoring.

This thesis proposes multiple algorithms applicable to unobtrusive pressure sensitive sensor arrays in order to assess sleep quality. These algorithms can be listed as adaptive movement detection, sensor data fusion and bed occupancy detection. This thesis also investigates long-term sleep pattern changes from previously recorded data. The methods developed in the thesis can be of interest for future clinical remote patient monitoring systems.

Acknowledgements

First, I would like to express my sincere gratitude to my supervisors, Dr. Martin Bouchard and Dr. Rafik Goubran for their invaluable support, instructive comments and guidance. Moreover, I would like to thank Dr. Frank Knoefel as my medical advisor and the person who developed the project and organized the collection of long-term data. I greatly appreciate his time and guidance throughout this work.

I also thank the financial support sources from Age-Well NCE Inc., Carleton University and admission scholarship from University of Ottawa for providing support and fund to accomplish this work.

I would like to thank my beloved sister, Dr. Sahar Soleimani who accompanied me in all pleasant and unpleasant moments throughout this journey. I know that it is a great honor that I have you as my sister, I am forever thankful to you. I specially would like to thank my father for encouraging me to fulfill my dreams. Words cannot express my deep heartfelt gratefulness to my mother for all her sacrifices, eternal love and caring no matter how far we were from each other. I am forever indebted to my parents for giving me opportunities and experiences that have made me who I am.

I wish to acknowledge my friends for their participation and help in my research. I appreciate your companionship in cheering me up whenever I needed it the most.

Last, I wish to extend my thanks to my dear god who empowered me to cope with the difficulties which I faced recently. Without the power that was re-granted to me, I would not have been capable to take this study to the end certainly.

Table of Contents

List of Figures

List of Tables

List of Acronyms

PSG: Polysomnography
REB: Respiratory Effort Band
PCC: Pearson Correlation Coefficient
BOS: Bed Occupancy Sensor
DRIP: Dual Respiratory Inductance Plethysmography
SDB: Sleep Disorder Breathing
AASM: American Academy of Sleep Medicine
OOC: Out of Center
SCSB: Statistic Charge Sensitive Bed
WISP: Wireless Identification and Sensing Platform
RF: Radio Frequency
SNR: Signal to Noise Ratio
PSD: Power Spectral Density
BPM: Breath per Minute
MRC: Maximal Ratio Combining
BR: Breathing Rate
HR: Heart Rate
BMI: Body Mass Index
UCL: Upper Control Limit
LCL: Lower Control Limit
MVDR: Minimum Variance Distortion-less Response
SFM: Spectral Flatness Measure

Chapter 1. Introduction

1.1. *Motivation*

Development of home-based technologies plays an important role in increasing older people's quality of life. Particularly, sleep monitoring is an active field of research as can be assessed by many new rapidly emerging technologies. Home-based sleep monitoring systems can reduce the inconvenience of using hospital-based ones and can provide immediate help whenever it is necessary. Wearable and non-contact health monitoring home-based devices have emerged to supply significant physiological information from their users in order to offer required emergency cares. There are many features that can be extracted through monitoring of patients in clinical or home-based settings such as bed occupancy, heart rate, breathing rate, skin temperature and movements. Breathing rate is one of the crucial physiological characteristics that can be identified with such technologies, and in case of sleep disorder its extraction could allow emergency needs to be delivered quickly. There exist many ways of performing unobtrusive non-contact sleep monitoring, as well as several obtrusive invasive ways of performing sleep assessment to capture physiological features of a patient.

Use of automated and unobtrusive sensors for physiological monitoring has become popular nowadays, since no devices need to be worn by individuals and it does not require any user interaction. It can address the need for sleep monitoring in a more effective real-time way and eliminate the cost of sleep monitoring in a hospital bed. Pressure sensitive sensor array is a non-contact unobtrusive device that has been validated to reliably perform patient monitoring. Therefore, a pressure sensor array can be placed below or on top of a mattress to extract

physiological features in an unobtrusive manner. However, when body movements occur, movement artifacts are introduced which can interfere with the breathing signal. Pressure sensors output a signal correlated to the exerted pressure produced by slight respiratory movements, the weight of a person lying on a mattress, and gross movements such as position changes. Therefore, signal processing methods can be applied to perform breathing signal extraction, motion monitoring, occupancy monitoring, central apnea screening, etc.

We aimed to carry out an investigation on validating and developing new algorithms for unobtrusive monitoring through bed-based pressure sensor arrays, in order to deliver quick health care in residential environments where early detection of crucial conditions can be difficult. The observation of sleep parameters variability on a long-term recorded data of people at their homes was the main focus of this thesis.

1.2. *Problem Statement*

As body movement is a source of impairment and interference in the signal obtained by the bed-based pressure sensor arrays, we are interested in detecting the time intervals in which the movements occur. Some research has used video cameras to detect movement. However, we are interested in less obtrusive movement detection tools by bed-based sensor arrays. One of the most effective unobtrusive methods to identify movement onset and offset times using pressure sensor arrays has been suggested by Holtzman *et al*. [1] based on a moving variance and a moving average of the pressure-sensor signals. In this research we propose some improvements to determine movement interval times with higher accuracy. Since movements interfere with the breathing signal, a higher accuracy is required in movement detection to diminish the corruptive effect of movements.

Thus far, techniques used to extract the breathing signal from mat sensors are mainly focused on free-of-movement periods of time, considering those movements as a corrupting factor for the breathing signal. In particular, instead of investigating the physiological characteristics of the individual lying on the mattress for the whole time, these methods merely identify the movements by different algorithms and mark the detected movement time as invalid, disregarding them for further investigation. Or, they use the previously developed movement detection method to minimize motion artifacts prior to apply breathing rate algorithms. Our goal is to estimate breathing rate during movement occurrences with acceptable reliability by using a new method of movement detection, so that movements can be identified and mitigated prior to rate estimation.

Many sensor signal fusion techniques were proposed in the literature to obtain breathing signal from pressure sensor arrays. We studied different signal enhancement methods to develop a new algorithm to perform noise, motion and interference cancellation. The novel method for combining the signals from the pressure sensors has been proposed and proved to have better correlation with a signal extracted from a respiratory effort band (REB) as a "gold standard" technique. The REB is a method of evaluating pulmonary ventilation by measuring the movement of the chest. The REB method was used concurrently with pressure sensor arrays to evaluate the extracted breathing signal from the pressure sensitive mat.

Aging can affect vital signs of individuals, as changes in body shape such as change in the chest wall and the shape of the diaphragm have an impact on the respiratory system. Therefore, in older patients, more studies need to be conducted in order to assess the changes in vital signs. We made a substantial effort in measuring older adults' quality of life by examining their data collected in a long-term basis which provided us a large volume of data (i.e., "big data"). We applied various methods on this big data to investigate older adults' breathing rate variabilities and bed activities.

This advancement is expected to help in the design of better algorithms for sleep monitoring to ensure health and autonomy of the older adults through more effective real-time actions in case of sleep disorder breathing. It is also hoped that the findings of this thesis will assist engineers to improve current sleep-pattern detection devices which is urgently needed by society.

1.3. *Research Methodology*

The main goal of this research was to observe long-term changes in sleep behaviours such as breathing rate, bed entry/exit patterns and bed occupancy of individuals with a special focus on elderly people. Figure 1.1 illustrates each of the four components of this research, which were designed to complement each other in order to achieve the main goal of this thesis.

1) In the first phase, we improved the previously available movement detection algorithm by using adaptive moving variance and moving mean signals to minimize motion artifacts. This method leads to estimating breathing rate with higher reliability during movement intervals.

2) In the second phase of this research, we studied different techniques for extracting the breathing signal and also a novel signal fusion method for breathing signal enhancement which outperformed other data fusion techniques.

3) In the third phase, we developed a novel occupancy detection algorithm based on finding the maximum distance among active sensors. The occupancy detection step was required in our research in order to minimize processing redundancy in long-term data processing (Chapter 8).

4) Lastly, in the fourth phase, long-term sleep assessment was performed by applying different algorithms on data captured from people at their homes, in order to observe vital sign changes over time.

All proposed algorithms were tested and validated using controlled experiments. Moreover, the approach for developing the algorithms was based on real-time analysis which is not dependent on future data. We assessed the performance of the proposed algorithms based on the Pearson Correlation Coefficient (PCC), some reliability metrics, and probabilities of false positives and true positives. The main platform for data conversion and analysis of recorded data was MATLAB (MathWorks©). All data were recorded using bed occupancy sensors (BOS) provided by Tactex Controls Inc.

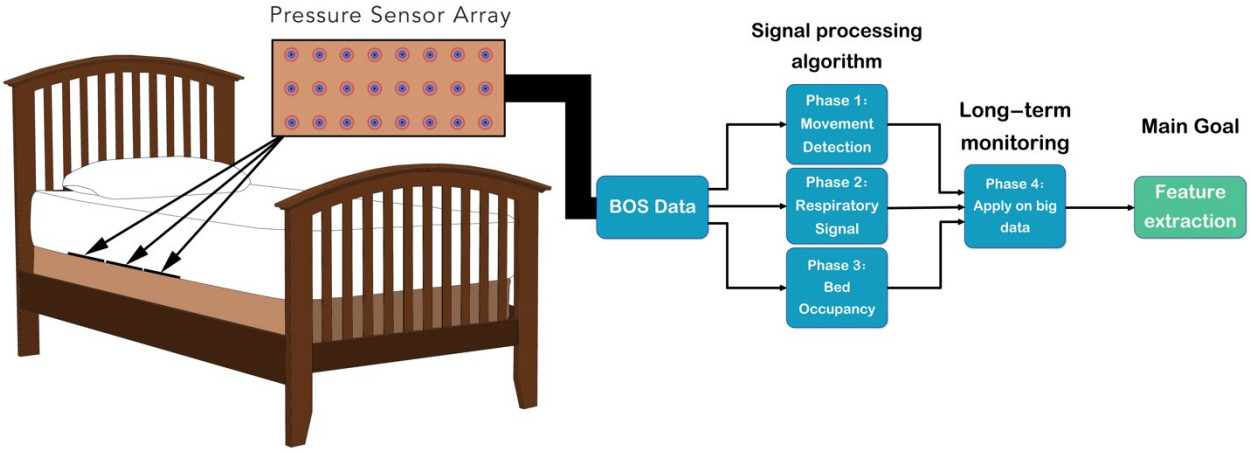

Figure 1.1. Four phases of this study including signal processing steps taken for feature extraction

1.4. *Contributions*

Contributions related to this thesis are listed as follows:

1. Constructed adaptive window length movement detection algorithm to identify movement onsets and offsets. This method was compared to the previous work on movement detection and results were published in [2]:

   S. Soleimani, S. Bennett, R. A. Goubran, H. Azimi, M. Bouchard and F. Knoefel, "Movement detection with adaptive window length for unobtrusive bed-based

pressure-sensor array," 2017 IEEE International Symposium on Medical Measurements and Applications (MeMeA), Rochester, MN, 2017, pp. 355-360.

2. Contributed to development of new pressure sensor signal fusion method based on beam-former theory to produce a higher quality breathing signal. This contribution was published in [3]:

   H. Azimi, S. Soleimani, M. Bouchard, S. Bennett, R. A. Goubran and F. Knoefel, "Breathing signal combining for respiration rate estimation in smart beds," 2017 IEEE International Symposium on Medical Measurements and Applications (MeMeA), Rochester, MN, 2017, pp. 303-307.

3. Introduced improved sensor selection method for respiratory rate estimation during movement. Results were compared to previous work in this field and were published in [4] and [5]:

   S. Soleimani, H. Azimi, M. Bouchard, R. Goubran, F. Knoefel, "Improved Sensor Selection Method during Movement for Breathing Rate Estimation with Unobtrusive Pressure Sensor Arrays," accepted with minor revisions for IEEE International Sensors Application Symposium (SAS 2018), Seoul, March 2018.

   S. Soleimani, M. Bouchard, R.A. Goubran, F. Knoefel, "Respiratory Rate Estimation by Unobtrusive Pressure Sensor Array during Movement", Students' Poster Day 2017, Medical Devices Innovation Institute (MDII) and NSERC CREATE "Biomedical Engineering Smartphone Training" (BEST), Ottawa, Sept. 2017.

4. Contributed to development of a method for apnea detection by Dual Respiratory Inductance Plethysmogrophy (DRIP), resulting in paper [6]:

   H. Azimi, S. Soleimani, M. Bouchard, R. Goubran, F. Knoefel, "Automatic Apnea-Hypopnea Events Detection Using an Alternative Sensor," accepted with minor revisions for IEEE International Sensors Application Symposium (SAS 2018), Seoul, March 2018.

5. Bed occupancy monitoring was also investigated. This work led to a novel method of occupancy detection measuring the occupied times where respiratory information is available.

6. Comprehensive investigation on bed occupancy, number of bed exits during day and breathing rate variability was performed on big data captured from several participants. Results obtained in this step will be submitted for publication in early 2018:

   S. Soleimani, M. Bouchard, R. Goubran, F. Knoefel, "Sleep Patterns Longitudinal Data Analysis from Pressure Sensor Arrays," in progress, 2018.

1.5. *Thesis Outline*

This thesis is divided into nine chapters which are presented in a chronological order as described below:

Chapter 1 presents the problems definition, general objectives, scope and the methodology of the research;

Chapter 2 covers a background review on wearable and non-wearable sleep monitoring technologies;

Chapter 3 defines different signal processing techniques which can be used to extract physiological features of bed occupants from bed-based pressure sensor arrays;

Chapter 4 describes the experimental setup including different sets of data collection that were made to examine the proposed algorithms;

Chapter 5 presents an improved movement detection technique to minimize motion artifact with higher precision;

Chapter 6 presents a new signal fusion method to generate a single output signal from pressure sensor arrays, and investigates the breathing rate estimation process;

Chapter 7 describes a new bed occupancy measurement technique based on the maximum distance in the active sensors;

Chapter 8 covers the relevant information for applying our proposed simplified algorithms on long-term home-based recorded data;

Chapter 9 provides conclusions in order to summarize the results, as well as suggestions for future research.

Chapter 2. Review of Sleep Monitoring Technologies

2.1. *Background*

In this chapter we provide background information on the use of wearable and non-wearable devices in sleep monitoring. We begin by introducing the gold standard test in sleep assessment called polysomnogrophy in Section 2.2, followed by presenting home-based technologies in Section 2.3. Moreover, a review will be made on unobtrusive sleep monitoring devices in Section 2.4. Finally, in Section 2.5 pressure sensitive sensor arrays (i.e., pressure sensor mats) will be presented as an unobtrusive tool in sleep assessment, which is the main method of data collection in the entire thesis.

2.2. *Gold Standard Test (PSG)*

Polysomnography (PSG) has been known and stablished by a committee of sleep researchers as the gold standard test for sleep disorder diagnosis [7]. PSG records several vital signs simultaneously during the whole sleeping period, such as chest and abdominal excursions, heart rate, and nasal airflow. Therefore, it has been used to study various sleep disorders such as sleep breathing disorders (SBD) including obstructive sleep apnea and central apnea, and movement disorders originating from grinding or clenching the teeth during sleep [8, 9, 10]. Recorded data by PSG will be interpreted based on rules presented by AASM [11].

While PSG is the most reliable diagnostic test in sleep monitoring, it faces the users with several challenges regarding obtrusiveness, invasiveness, accessibility, expenditure and dependency on special polysomnographic technologist. The user needs to travel to hospital or a sleep laboratory

for data collection, which is costly. Moreover, respiratory effort bands (respi-bands) and oronasal airflow sensor must be fitted and worn for the entire data recording. Therefore, despite the reliable utility of PSG, some patients are reluctant to undergo the entire testing process.

As sleep behaviour changes from night to night, monitoring of vital sign variations for only a few nights is not valuable for clinical interpretation. While the laboratory PSG is encountered with certain limitations for the sake of longitudinal sleep analysis, home monitoring devices are capable to provide physiological monitoring for an unlimited period of time. So the major issues of inconvenience and cost have motivated researchers to develop devices capable of sleep assessment in real-life condition such as home environments. Therefore, demand for alternative sleep monitoring devices arises, particularly to overcome the issues related to wearable clinical sleep monitoring technologies.

2.3. *Home-Based Sleep Monitoring Technologies*

Although the gold standard test for sleep evaluation remains the laboratory polysomnogram, there is an increasing demand in using portable devices to acquire sleep information in non-clinical environments such as home. These devices provide self-experimentation and evaluation with no user interaction to interpret and investigate the data. Furthermore, they bring comfort for patients as they no longer need to stay in hospital to be examined by clinical-based devices, which is very disruptive and expensive.

The use of several home-based sleep tests has been evaluated and reviewed in research studies [12, 13], helping clinicians to decide about the adequacy and sufficiency of data resulting from various out-of-center (OOC) devices, particularly in the diagnosis of obstructive sleep apnea. Kelly *et al.* reviewed recent developments on home-sleep-monitoring devices [14]. They investigated various devices which are potential candidates to render home sleep assessment. She categorized

numerous devices based on the way they perform data collection. Some devices capture the data according to brain activity signal such as iBrain and Zeo devices, whereas some others collect sleep information based on movement such as Fitbit and Lark devices. She also mentioned bed-based sleep monitoring devices which is in the realm of this thesis.

Verrier *et al*. reported that 15% of sudden deaths and 20% of heart attacks occur from midnight to 6 AM [15]. Therefore, timely detection of unexpected situations happening during sleep is quite important. They elaborated the need of home healthcare services for several groups of patients with high risk of nighttime incidents, requiring real-time identification with minimal impact on their sleep quality. In general, older adults are at higher risk of sleep disorders compared to younger ones, and this leads to nocturnal cardiorespiratory problems. Also, patients newly released from hospital require sleep monitoring to avoid of reoccurrence of their abnormal breathing events. Hence, it is desired to have accessible and feasible technologies for online monitoring of sleep related respiratory risks which are available in home environments. In addition, equipping such devices with alarm features will assist the caregivers to intervene and deliver the necessary aid services instantly when it is needed. Therefore, unattended portable devices providing self-monitoring mechanism to patients at home can play an important role in consumer acceptance and saving the lives of many people.

2.4. *Unobtrusive Home-Based Technologies*

Privacy has been found to be an important requirement for patients using home sleep monitoring devices [16]. Privacy concerns prevent people from sharing their daily activities with interpreters, researchers or clinicians in trade of health benefits. So, they avoid adopting all kind of home sleep monitoring technologies. This adoption relies on a trade-off between autonomy - which is obtained by accepting the sensor - and privacy which is compromised by the use of the sensor itself.

There is rapid development in emerging various unobtrusive home-based sleep monitoring devices which have been found to be more admissible by patients. There are many unobtrusive systems reported in the literature for measurement of physiological information. Beattie *et al*. evaluated depletion of load cell underneath the legs of the bed in detecting apneas and hypopneas [17]. Prior to his work, some studies had also been performed to validate the capability of load cell sensors for detection of vital signs such as heart rate and respiration rate [18, 19]. The load cell sensors collect data automatically based on the amount of weight changes in each leg of the bed with no interference on the patient's sleep. Some researchers have also used these sensors in order to track the movement of a bed-occupant during the night as well [20]. The strain gauge transducers used in load cell technology convert applied weight into resistance change. The problem of this system is in the difficulty of its mounting and set up.

Static charge sensitive beds (SCSB) make use of metal plates embedded in a mattress which capture induced charges produced by movement in bed [21]. This leads to generating a single electrical signal reflecting a bed-occupant's features such as breathing rate, body movement and ballistocardiogram. Jansen *et al.* investigated the extraction of heart rate through ballistocardiogram detection of signal obtained from SCSB [22]. Polo *et al.* validated the application of SCSB in detecting obstructive apnea occurring during sleep [23]. SCSB operates by capacitor sensor whose non-linear response and hysteresis were reported as their main disadvantages.

The researchers in [24] used wireless identification and sensing platform (WISP) tags attached to bed mattress for sleep monitoring purposes. WISP tags extract accelerometer data which can then be analyzed in order to distinguish body positions and movements during sleep. Despite the tremendous advantages of WISP tags such as low cost and unobtrusiveness, they are not sufficient

for professional sleep monitoring. For instance, WISP tags themselves all alone do not provide information regarding breathing rate or heart rate.

2.5. *Pressure Sensitive Sensor Arrays*

Non-invasive unobtrusive bed-based pressure sensitive sensors have been introduced as a significant component in medical monitoring [25]. Holtzman *et al.* investigated the effect of mattress type and its thickness in order to validate pressure sensitive sensor mats for physiological monitoring [26]. In particular, the unobtrusive nature of pressure sensor mats enables researchers to obtain longitudinal sleep information with no significant cost. In fact, it brings possibility of performing sleep assessment for patients while they are in bed with no discomfort and obtrusiveness. To ensure that this technology is successful in performing sleep monitoring, it requires a performance evaluation for the quality of delivered content. Townsend *et al.* validated the capability of pressure sensitive sensor arrays in central sleep apnea screening [27]. She also made a substantial effort in developing enriched algorithms to detect central apnea exploiting pressure sensor arrays [28, 29, 30].

Pressure sensor arrays can be used to identify sleep information including breathing signal extraction [31], movement detection [1, 2] and breathing rate estimation [4, 32]. Pressure sensors in these arrays output a signal correlated to the exerted pressure produced by slight respiratory movements, the weight of a person lying on a mattress, and gross movements such as position changes [33].

The fundamental purpose of sensory device is to produce a signal which enables the well-being of a patient to accurately be determined. Pressure sensor systems have recently been used in order to monitor physiological signals of sleeping subjects. There exist numerous types of pressure sensors in the literature that can sense the pressure and generate a related signal in the output. The

embedded sensors in the commercial pressure sensor arrays used in this thesis take advantage of fiber optic technology which is highly sensitive to slight bends; this sensitivity enables users to situate the sensor array beneath the mattress, leading to an unobtrusive sleep monitoring tool. In addition to their durability feature in case of heavy loads, these kinds of sensors can be acquired at a relatively low price. Using multiple sensors in an integrated array provides load distribution information of the pressure applied from particular coordinates over the patient body. This allows creating a pressure image or video.

The Kinotex pressure sensor is a member of the fiber optic pressure sensor family which exploits the fiber optic principle in its configuration. The Kinotex fiber optic pressure sensors modulate light instead of an electrical signal. This technology protects the fiber optic sensors in case of exposure to radio frequency (RF) signals [34]. The validity of using Kinotex sensors has been provided by Sakai *et al.*; comparison results with an existing pressure sensor indicated that it can be considered as a valid instrument for clinical use [35]. The most important feature of this kind of sensor is that it is cost-beneficial with low dependency on temperature changes [36].

The Kinotex sensor is comprised of two plastic optical fibers as its sensing elements, constructed in a non-linear foam structure. These two plastic layers are responsible to transmit and receive the light reaching it. The emitted light from a light-emitting diode is sent to the sensing point by the transmitter fiber and it is received by a photodiode through the latter fiber. It operates by detecting the power intensity of the scattered light. When pressure is exerted on the foam, the intensity of this light will be increased. The photodiode measures the received light, then converts it to a voltage proportional to the applied pressure. Therefore, the sensed force can be estimated by creating an inverse model to convert the voltage back to the applied pressure [37]. The internal structure of the fiber optic pressure sensor is depicted in Figure 2.1.

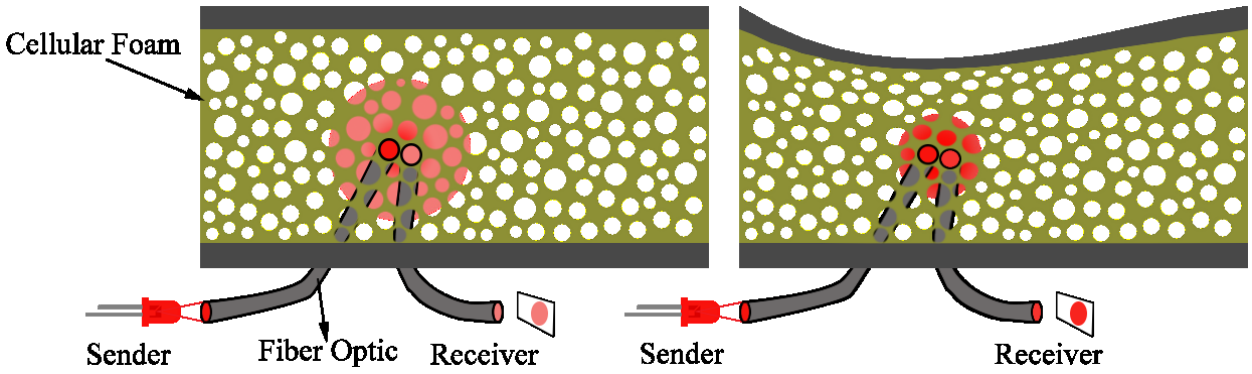

Figure 2.1. Kinotex sensor

As can be seen in the right part of Figure 2.1, the fiber optic sensor foam is deformed due to the pressure applied on it. This deformation causes higher intensity in the light conducted to the receiver.

Chapter 3. Previous Studies with Pressure Sensor Arrays

Pressure sensitive sensor arrays are met with greater acceptance among other home-based sleep monitoring devices, more specifically for the patients dealing with cognitive or physical troubles. In addition, these devices are more preferable in long-term health information data collection as they remove some of compliance issues associated with contact sensors. This device provides significant information regarding patients' health properties as discussed in this chapter. Some state-of-art methods that researchers have done to extract these properties are also described in this chapter.

3.1. *Data Fusion Techniques for Extracting Respiratory Signal*

One of the most important information captured by pressure sensor mats is the respiratory signal. Positioning pressure sensor arrays underneath the mattress allows them to be used to acquire breathing signal, which can be further investigated to determine other information such as apnea detection and breathing rate. For finding the breathing signal, researchers used various filtering methods to extract the frequency range of interest. Filtering removes unwanted components from the sensor signal that is being measured.

Use of a sensor array instead of one single sensor provides the opportunity of combining sensor signals to create a single breathing signal with a better quality, i.e., a better signal to noise ratio (SNR).

This section presents previous work in the domain of breathing signal extraction methods.

3.1.1. *Reference Sensor Signal Method*

Previous research in finding respiratory signal by sensory technology showed the capability of a single sensor in determining breathing rate [38]. Therefore, the strongest sensor in the pressure mat can be selected as the reference sensor and further feature extraction can be performed from this sensor. This selection can be performed based on different criteria. Some used the signal with the greatest average power in time domain, whereas others considered reference signal as the sensor signal exhibiting highest power in the frequency band of interest. In the latter one, scoring would be performed on sensor signals based on their relevant SNR in the spectral power density in the breathing frequency range. Sensor signals with high SNR include a peak in their power spectral density (PSD) in the desired frequency band. The respiratory rate is then estimated on the selected sensor with highest frequency score. Nishida *et al.* chose a sensor signal whose power spectrum density is the largest in a desired frequency band (0.25 Hz to 0.33 Hz) as a reference sensor signal; they assumed that normal breathing rates range from 15 to 20 breaths per minute (BPM) for healthy individuals [39].

Holtzman *et al.* proposed a new method of choosing the reference sensor signal and its performance was compared to two other methods [40]. Comparison was made after minimizing movement artifacts with available movement identification algorithms [1]. She concluded that although her proposed method presented better outcome, overall there was only a slight decrease of performance in the other two methods.

In general, the selection of a single signal is likely to result in error, particularly in the presence of interference or noise sources. Therefore, it is a good practice to use data fusion in conjunction with a reference sensor instead of using only a reference sensor signal.

3.1.2. *Delay and Polarity Correction*

Depending on the sensor locations with respect to distance from the chest or abdomen area of the subject lying on a bed, their respiratory effort information may vary. They may contain more information when they are directly situated beneath the chest and abdomen compared to when they are placed further away, as they may capture no or little information about slight respiratory movements. Therefore, applying a fusion method will help in generating a single output signal with better quality.

Adding all polarity-corrected sensor signals together to produce a single output is one method of data fusion technique. Polarity correction is one of the important attributes of array signals required to be conducted prior to or as part of data fusion. It is applied in a number of data fusion algorithms. This step is performed in order to align sensor signals with reversed polarity compared to the reference sensor signal, due to the fact that the loading effect varies from sensor to sensor, where increasing load on one sensor simultaneously can decrease the load from another sensor. This method was used in [41] in order to obtain breathing-related signal. The reference sensor signal selection was based on Nishida et al.'s method [39]. Then the Pearson Correlation Coefficient (PCC) was chosen as a tool to compare the similarity of the reference sensor signal to all other sensors. Indeed, the sign of the PCC is sufficient to elicit whether a sensor signal is in phase with the reference sensor signal or if it is out of phase with it. If this sign is positive, then it is assumed that they were both in same slope direction and no correction is required. However, a negative sign indicates that they are in different directions (one is falling while the other is rising) and polarity correction is required.

PCC between the k^{th} sensor signal and the reference signal is calculated based as follows:

$$r_k = \frac{\sum_{i=1}^{M}(c_r(i)-\bar{c}_r)(c_k(i)-\bar{c}_k)}{\sqrt{\sum_{i=1}^{M}(c_r(i)-\bar{c}_r)^2}\sqrt{\sum_{i=1}^{M}(c_k(i)-\bar{c}_k)^2}} \quad (3.1)$$

where c_r is the reference sensor signal and c_k is the k^{th} sensor signal. Note that if only the sign of the PCC is used for polarity adjustment, then the denominator does not need to be computed, as it is always positive.

It is worth mentioning that the polarity reversal works well in the situation that the signals are not corrupted by movement. During movement, the reference sensor signal selection may result in detecting the one most affected by movement artifacts, with little or no information about breathing. Also, the sign of PCC may be disrupted by movement occurrence. For instance, two sensor signals might be out of phase during normal breathing, while they might be in phase at the time of movement event. Such situations might lead to positive PCC rather than negative PCC because of extreme values of movement samples [41].

Movement detection algorithms can assist researchers to minimize movement artifacts in a way that movement samples could be identified and be discarded for further investigation, or movement suppression techniques could be used to minimize the movement corruptive effects. This way, polarity reversal technique would be immune in case of movement interference, although there still exists other corruptive factors caused by noise or drift that may impact the performance of the polarity reversal method.

The second important signal attribute is delay. The delay may be generated either because of breathing characteristics or by asynchrony in transferring the applied pressure to sensor elements. Holtzman [41] inspected the effect of signal inversion in data fusion whereas Townsend *et al*. also

investigated the effect of signal delay in addition to the effect of polarity reversal [42]. The latter work did the correction in two steps: first polarity correction and second delay adjustment. All polarity delay corrected signals were summed up to build the breathing signal. The cross-correlation parameter at lag zero was used instead of PCC (i.e., discarding the denominator which brings no information) to compare the reference sensor signal with all other sensor signals in order to correct the polarity. The reference signal was chosen based on the maximum amplitude in the sensor signals, which were estimated through signal properties such as valleys and peaks. After aligning the polarity, the existing delay in all sensor signals was adjusted by comparing each sensor signal with the reference sensor signal using cross-correlation with a lag up to plus/minus 1 second. The breathing signal quality obtained by the three aforementioned methods was assessed by comparing signal amplitude and SNR where it was shown that the signal with both polarity and delay correction had the highest SNR and signal amplitude [43].

Figure 3.1 illustrates the temporal difference among the three different models of breathing signal extraction. These signals were captured from 30 seconds of a data free of movement. In order to compare the performance between the methods, SNR or PCC computations can be used (depending on the application). In Chapter 6, a comparison among the methods is performed based on the PCC calculated for each of the method, with a gold standard measurement method. All algorithms were performed in an epoch by epoch basis (period of 30 seconds).

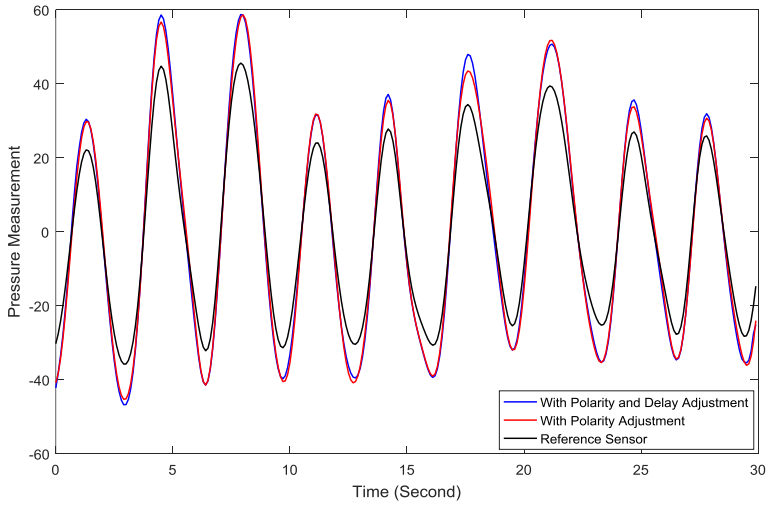

Figure 3.1. Breathing signal captured by three different methods

3.1.3. *Maximal Ratio Combining Method (MRC)*

Signals collected by sensors are functions of time. Time domain signals can reveal enormous amount of information regarding the state of a subject. Similarly, data combining techniques can also be constructed by looking at specific properties of frequency domain signal.

The Maximal Ratio Combining (MRC) method is a technique for sensor signal fusion which can be applied on sensory data to yield the breathing signal. This method is applied after correcting all signal polarities with respect to the reference sensor signal. There is a weighting factor required to be built for each sensor signal based on noise power and signal power estimates. It is constructed for all sensor signals in order to sum the signals with respect to these factors. Therefore, this method aims to weight the sensor signals with optimal gain factors.

The required estimates for constructing the gain can be calculated with various methods. Two different methods named MRC VAR and MRC PSD were investigated and compared in [44]. MRC VAR uses the variance of the temporal signal in order to estimate the noise and signal power

parameters, while the MRC PSD computes the power spectral density in order to estimate these parameters.

3.2. *Movement Detection*

Motion artifacts can lead to devastating signal quality losses, which cause serious obstacles in the reliable use of any sleep monitoring devices, particularly pressure sensor arrays for breathing rate extraction. Various signal processing techniques have been implemented to address the issues originating from movements and removing its corruptive factors.

Some research has used cameras to compensate for movement on a real-time basis by applying image sequence analysis [45]. Facial feature tracking using computer vision algorithms is the fundamental basis for movement compensation by camera. However, patients are reluctant to undergo video capturing for real-time analysis since it does not preserve their privacy. Moreover, the algorithms have some vulnerabilities in case of motions with large variations.

Pressure sensor array outputs are highly disrupted by movements. Therefore, to estimate breathing rate reliably we must minimize the corruption caused by motion artifacts. Movement onset and offset detection by pressure sensor arrays was investigated in [1]. This algorithm works by setting an upper and a lower control limit in order to detect movement intervals. The two control limits are constructed based on the moving variance and moving average estimates. The detection process is followed by meeting some conditions at a certain number of sensor signals. Onset detection is conducted by finding any two consecutive samples below the lower control limit or above the upper control limit. The detected movement is continued for the subsequent samples and it will be considered to end when the amount of change in two adjacent samples is negative in the upper control limit. Moving variance and moving average are implemented by sliding a fixed

window over time on all sensor signals to obtain variance and mean estimates updated on a sample by sample basis.

3.3. *Bed-Occupancy Monitoring*

In the past, restraint-based patient treatment was common-place in patients prone to falling. This strategy is based on restricting the movement of a patient so that he/she would no longer be at the risk of falling. However, researchers have shown that this method can be more noxious rather than being advantageous. Therefore, they decided to come up with sensor-based occupancy monitoring devices in order to detect emergency falling cases which do not intervene with their sleep.

Bed occupancy monitoring by pressure sensitive sensor arrays provides an unobtrusive measure for tracking bed exit/entry patterns of patients. Presence or absence of bed occupant reveals significant information about the total time that people spend in the bed. This information allows clinicians to examine sleep quality with the potential of identifying critical changes in health status and mobility. Particularly, it becomes useful for monitoring an infant occupancy in order to minimize the risk of falling.

In addition, in big data processing, bed occupancy algorithms are required to decrease the complexity of process as we can eliminate the portion of data recorded for the time no one occupies the bed. This way, the further processing techniques can avoid being used for those periods of time, which results in cost and time saving.

There exist some occupancy detection methods applicable to sensor arrays that researchers have previously implemented. In the following, the two models recently presented in the literature are described in detail.

3.3.1. *Occupancy Detection by Finding Loaded or Active Sensor Method*

This occupancy detection method is based on the principle of finding at least a certain number of sensors as occupied (S_{occup}), in active or loaded status [41]. The detection is based on exceeding a pre-set threshold. Holtzman [41] used this method in her work in order to observe weight distribution in case of movement. This strategy is based on considering a sensor as occupied if and only if it is detected as loaded or active. In order to find out sensor status, a sliding moving average and a moving variance are used. To identify sensor activity, a pre-set threshold was imposed as h_{act}, such that if the standard deviation passes this threshold the sensor is announced as active. h_{act} was chosen as 2% of the maximum possible value of the sensor. Loading was detected if the moving average exceeds h_{zero}, corresponding to the minimum value between 110% of the smallest value recorded in the full data or 20% of the maximum value that the pressure sensor is able to tolerate. The minimum required number of sensors for declaring occupancy was chosen as 40% of the total number of sensors.

This method is not recommended to be used in case of bed entry/exit detection, as it will result in low sensitivity. For instance, the bed occupant might exert pressure on the bed with only his or her hands without occupying the bed; then as soon as he or she takes off the load the method detects bed exit, which is not an actual exit. Therefore, this method is more beneficial in exhibiting load distribution, especially for demonstration of pressure sensor images and videos as in [41].

Therefore, new techniques are required to be developed in order to measure sleep metrics including duration of bed exit and bed entry, sleep start time and sleep end time with higher sensitivity.

3.3.2. *Threshold-Based Occupancy Detection According to Height and Weight of Bed-Occupant*

Analyzing occupancy can be performed in a way to be applicable for all mattress types and people's anthropometric characteristics. This algorithm is based on establishing a threshold by combining the pressure sensor base value and the bed-occupant's weight parameter [46]. This threshold can be adjusted in order to obtain the sensitivity required depending on the type of application.

We applied this method in our big data processing with a small modification in order to get rid of the large number of hours of useless data recording. As the information about the patients' weight was not available, the technique was adapted to be compatible for all types of patients with no prior information about them. This will be further described in detail in a later section.

Chapter 4. Experimental Setup and Data Collection

This chapter provides information about the experimental set-up used for data collection in addition to the types of uncontrolled and controlled experiments respectively used to perform sleep assessment and to validate the corresponding algorithms. Moreover, the devices used to extract sleep patterns are also presented with relevant characteristics.

Since all experiments involved human participation to capture pressure data from people with different ranges of height, weight and age, ethics approval was obtained from the University of Ottawa Ethic Research Committee and Carleton University Ethic Research Committee prior to new data collection or analysis of previously recorded data. Moreover, consent forms were provided to volunteers to be signed before starting experimentations.

4.1. *Experimental Setup*

The equipment used in this research for sleep parameter extraction was: a) white pressure sensor mat, b) black pressure sensor mat and c) Zephyr Bioharness wearable chest belt as depicted in Figure 4.1. Two types of data recordings were used in this thesis; short-term and long-term data recording. Short-term data collection was conducted in two categories: short-length and nocturnal data recordings. The objective of conducting short-term data collection was to design algorithms parameters and to evaluate the performance of implemented algorithms. Short-term data were collected by the author of this thesis and all participants were healthy adults ranging from 22 to 70 years old, whereas long-term data were collected by previous researchers from seniors (mostly in their 80s) living in their homes.

Short-term data recording experiments were performed in a controlled setting to achieve robust algorithms. Later on, the simplified versions of these algorithms were used to further analyze the big data, which was previously captured from uncontrolled experiments for sleep quality assessment.

a) White pressure sensor mat

b) Black pressure sensor mat

c) Chest belt

Figure 4.1. Sensory equipment used for measurement

4.1.1. *Bioharness Chest Sensor*

In order to validate the algorithms for breathing signal extraction, results were compared to a reference which was very similar to the gold standard polysomnography. Therefore, the Zephyr Bioharness chest sensor was used as a reference along with the pressure sensor in a controlled experiment for evaluation purposes.

The Zephyr belt sensor is capable of measuring numerous physiological characteristics such as skin temperature, breathing rate (BR) and heart rate (HR). This sensor collects the results every second and saves them in a .csv text format file.

The accuracy of this device for the measurement of heart rate and respiratory rate information has been previously examined by other researchers [47]. The examination was conducted during two graded and sustained exercise protocols; results were compared to a standard laboratory system and a previously validated portable device in order to evaluate the use of the Bioharness chest belt. Findings of this study revealed that the Bioharness sensor is capable of providing reasonably accurate HR and BR with no significant difference from the two aforementioned devices. Therefore, it can be used as a gold standard in our work instead of standard laboratory polysomnography.

4.1.2. *Pressure Sensor Mats*

Both types of mats used in this study were manufactured by Tactex Control Inc. Each sensor array has 24 evenly spaced fiber optic pressure sensors in a 3x8 framework. The pressure-sensitive area of this array was approximately 80 cm by 25 cm and the sensors were evenly spaced 10 cm apart. The pressure sensor made of optical fibres receives the applied pressure and outputs a voltage proportional to the exerted pressure. The output voltage is then sent to a Bluetooth box via a wire and is transmitted to a computer. Afterwards, the MAT software in the computer receives

the voltage information, converts it to nominal scores and then stores the data in comma separated files.

The main difference between the black mat and white mat is in the number of samples they store per second; i.e., sampling rate. The black mat has been designed to store 20 samples per second (20 Hz) whereas the white mat captures 10 samples per second (10 Hz). Also, the black mat used in this research consisted of three concatenated pressure sensor arrays with 72 sensors in total and the white mat is comprised of only one sensor array (24 sensors). All data were captured by the data acquisition software provided by Tactex Control Inc.

4.2. *Controlled Experiments*

For the purpose of performance evaluation and design of algorithm parameters, the use of controlled experiments was necessary. In the following, the controlled experiments used in this study are explained in detail.

4.2.1. *Controlled Experiment Used for Movement Detection Algorithms*

Pressure sensors output a signal correlated to the exerted pressure produced by slight respiratory movements, the weight of a person lying on a mattress, and gross movements such as position changes. Figure 4.2 shows some typical sensor signals under different conditions.

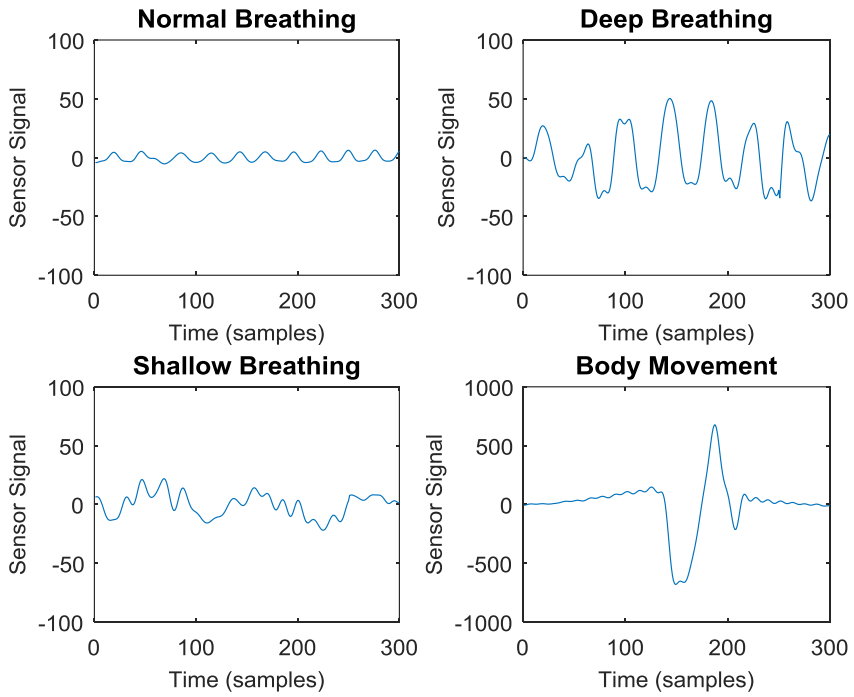

Figure 4.2. Typical sensor signals under different conditions

In the experiment of movement detection discussed in Chapter 5, a white Tactex Controls Inc. Bed Occupancy Sensor (BOS) array was placed horizontally underneath a mattress along the bottom of the pillow area.

Two different types of data were collected. First, 20-minutes long data were collected from five healthy volunteers, 3 males and 2 females ranging from 22 to 38 years old (volunteers #1 to #5 in Table 4.1). They were asked to lie on top of a mattress with different postures to perform different actions of movements and sleep patterns, such as deep breathing, shallow breathing, normal breathing, breath holding, head movement, arm movement, rollover, position changes and other random types of movements. Second, nocturnal data were collected overnight from two subjects, a male of age 31 and a female of age 36, volunteers #6 and #7 in Table 4.1. Recording was started from the time they went to bed till the time they got out of bed, with a length of 6.73 hours and 7.42 hours, respectively. The location of the sensor array remained the same for the entire data

collection duration. Actual start and end times of all events were precisely annotated by the investigator during the entire period of data collection, in a time stamped log file. Table 4.1 presents some anthropometric information relevant to all seven volunteers, including in particular the volunteers' weight and height.

Table 4.1. Anthropometric information of the study participants

Volunteer #	Gender	Height (cm)	Weight (Kg)
1	M	168	69
2	F	156	55
3	M	185	79
4	M	171	68
5	F	163	70
6	F	170	65
7	M	182	78

4.2.2. *Controlled Experiment Used for Breathing Signal Extraction and Breathing Rate Estimation Algorithms*

There were two types of data collected for this experiment: nocturnal data conducted to estimate breathing rate during movement and also short-length data to validate the improvements in the proposed SNR-max data combining method [3] were as follows. A white bed-based pressure sensor array consisting of 24 sensors was placed beneath a mattress. This array is manufactured by Tactex Controls Inc. and is in a configuration of three rows of eight sensors. Figure 4.3 shows the experimental setup of sleep monitoring using this sensor array.

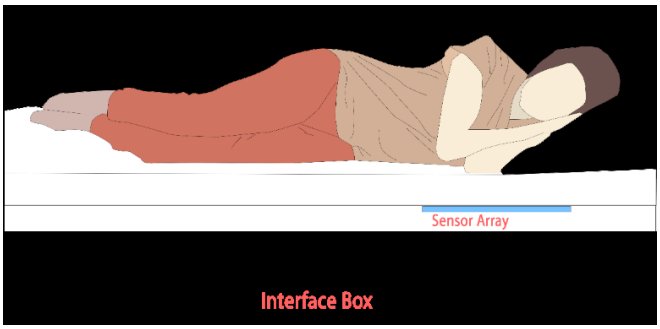

Figure 4.3. Measurement Setup

The output of the pressure sensors is proportional to the force exerted on it. As mentioned in Section 4.2.1, this force also includes slight respiratory movements; therefore, we can estimate breathing rate from the pressure sensitive sensor array.

To this end, nocturnal data were collected from healthy female and male subjects. They both spent a whole night with the bed pressure sensor array under their mattress in a completely unobtrusive way and without any interference with their sleep. The male subject spent 6.83 hours, and the female 7.51 hours in bed. Data collection was started from the time they got in bed till the time they got out of bed. The male subject was awake for a while after spending 5.86 hours in bed; then he again fell asleep for the remaining time, and as soon as he woke up he left the bed quickly. The female subject returned to her waking consciousness after spending 6.71 hours in bed. She stayed awake in bed for the remaining time till she got out of bed. The female subject had a weight of 64 kg and a height of 170 cm, the male subject had a weight of 79 kg and a height of 185 cm.

Although a respiratory band (respi-band) is the most reliable device in determining and tracking breathing rate, it can be considered obtrusive, invasive and inconvenient for the users. Moreover, it is vulnerable and prone to gross movements. Therefore, for comparison of respiratory rate measurements obtained by different approaches for periods including movements, no data collection was performed with respi-bands. This is because we intended to improve breathing rate

estimation during movement, and as it was mentioned earlier respi-bands were found to be very sensitive to gross movements, specifically those originating from position changes. Therefore, we will evaluate the performance of our proposed method based on a reliability metric and using the mean and variance of breathing rate estimates. However, to show that our proposed SNR-max combining method from [3] outperforms other methods in terms of obtaining better signal quality, we collected a set of 5-minutes long free of movement data from five healthy volunteers ranging from 24 to 70 years old and wearing a respi-band. The volunteers were asked to lie in bed in supine position with no movement for the entire data collection. The first two participants were tested with a black mat consisting of 72 sensors with sampling rate of 20 Hz (3 arrays, each with the same configuration as the 24 sensors array) and the rest were conducted with the same bed occupancy sensors used in the previous experiment. Evaluation was made based on computing the Pearson Correlation Coefficient between the signal extracted from the respi-band and the signal obtained from different data fusion methods.

4.2.3. *Controlled Experiment Used for Bed Occupancy Detection Algorithm*

The validation set used in Chapter 7 is comprised of 5 approximately 12-minute long recorded files collected from five participants. They were asked to follow a same script including performing breathing in supine, prone and side positions as well as imitating hard sit to stand transfers as real patients, sitting and relying on the back of bed imitating reading position. This experiment was repeated for five healthy volunteers. With the max-distance occupancy method described in Chapter 7, we aimed to detect only the times when the sensors can sense the available respiratory movements instead of all occupied periods of times. That way, we can further reduce the complexity of breathing signal analysis, since the recorded data with lack of breathing motion such as sitting and reading periods will be eliminated in the data processing.

The black pressure sensor mat consisting of 72 sensors equally spaced in an 8 by 9 grid array was used for this experiment. As mentioned earlier, pressure values at the sensors are recorded every 0.05 s (20 Hz) in this mat.

All the controlled experiments conducted in this research were performed by healthy volunteers with normal body mass index (BMI), which may cause limitations in the applicability of the developed algorithms. For instance, the pressure sensors saturate at a certain value, where the changes above that value cannot be captured. This certainly can happen for heavier people with high BMI. On the other hand, for people with low BMI, there might be a problem of sensing changes of breathing amplitude in different breathing patterns using pressure sensors, as these changes could be very subtle for this category of people.

4.3. *Uncontrolled Experiments*

Simplified methods were applied to long term big data recorded from older adults at their homes for a period of time ranging from 101 to 397 days, with three different configurations as follows. Some recordings were performed by three white mats placed side-by-side, some by a single black mat and a few with a mixed configuration as described in Table 4.2. All mat sensors were placed horizontally underneath the mattress. A MATLAB script was written to analyze the data and to be compatible for all three data recording configurations. Information regarding the patient numbers or IDs, start/stop day of data recording and the data collection mat format is provided in Table 4.2.

Table 4.2. Big data recording information

No.	Participant No.	Total Number of Days of Recording	Type of Mat	Start Day	Stop Day
1	MD 116	152	Black pressure sensor mat	2013-06-06	2013-11-03
2	MD 139	126	Three white pressure sensor arrays	2013-06-07	2013-11-08
3	MD185	295	Three white Pressure Sensor Arrays	2013-07-10	2014-06-29
4	MD 202	101	Three white pressure sensor arrays	2013-09-03	2013-12-12
5	MD 206	397	Black pressure sensor mat	2013-11-06	2014-02-25
			Three white Pressure Sensor Arrays	2014-04-16	2015-01-26
6	MD 226	110	Three white Pressure Sensor Arrays	2013-12-02	2014-03-21
7	MD 231	306	Black pressure sensor mat	2013-11-26	2014-07-29
			Three white Pressure Sensor Arrays	2014-07-29	2015-01-20
8	MD 442	239	Black pressure sensor mat	2013-11-25	2014-05-28
			Three white Pressure Sensor Arrays	2014-06-11	2014-12-19
9	MD259	204	Three white Pressure Sensor Arrays	2014-02-06	2014-12-19

In order to assess sleep quality, the pressure data were analyzed on a day-by-day basis for a period of 24 hours. The extracted information was also displayed with the same format longitudinally. A batch file was written and applied on the big data to reduce the loading time of the .csv files. Upon loading the .csv files, the script concatenates all related files belonging to a specific day. We chose a duration from noon to noon for dividing data into days. For data storage efficiency, each noon-to-noon daily data was stored as a binary file. A binary storing format had some benefits such as less memory usage and storage size, as well as faster reading time. This approach was used to read the big data available for this study.

Chapter 5. Adaptive Movement Detection Algorithm

In this chapter, the implementation of the adaptive movement detection algorithm published in [2] is described in detail. This algorithm was used to determine movement interval times by sliding an adaptive window over time on a reference sensor signal, to obtain variance and mean estimates updated on a sample by sample basis. In Section 5.1, the algorithm is described in detail, followed by performance evaluation of this method presented in Section 5.2. The chapter is concluded in Section 5.3.

5.1. *Proposed Method*

5.1.1. *Preprocessing*

The data captured under the controlled experiment explained in Section 4.2.1 was used in order to analyze the performance of the proposed movement detection algorithm and also to design algorithm parameters.

The raw data was first segmented into 30-seconds epochs to conform with the standard in sleep analysis and to be able to take real-time actions in case of detected sleep disorders. Further processing was made on an epoch by epoch basis. A band-pass filter with low and high cut-off frequencies of 0.07 Hz and 0.8 Hz was applied for each epoch on all 24 sensors, to remove the effect of static weight of the bed occupant and to focus on the breathing frequencies. The reason for working in the respiratory frequency range is because the goal of detecting movements was to mitigate its corrupting effects on the breathing signal.

Afterward, the reference sensor was selected in each epoch among the 24 sensors, based on the maximum average power, and reference signals for each epoch were concatenated over time to

yield a signal $x(k)$ for further processing. In the following, we elaborate in detail how to process this signal in an on-line fashion suitable for real-time processing.

5.1.2. *Adaptive Window-Length Moving Average and Moving Variance*

In order to determine the movement interval times, we made two signals from $x(k)$: a moving average and a moving variance signal. Both of these signals were constructed by a window sliding through time and calculating the mean and variance on a sample by sample basis. $\mu_x(k)$ and $\sigma_x^2(k)$ denote the moving average and moving variance signals, respectively, which were obtained as follows:

$$\mu_x(k) = \frac{1}{W(k)} \sum_{i=k-W(k)+1}^{k} x(i) \tag{5.1}$$

$$\sigma_x^2(k) = \frac{W(k)}{W(k)-1}\left(\mu_{x^2}(k) - \mu_x^2(k)\right) \tag{5.2}$$

where $W(k)$ is the length of the sliding window. As can be seen, the window length was allowed to be adaptive and vary with time. Unlike a fixed window length as in [1], an adaptive window length can be more efficient in movement detection when the consecutive movements occur in a time shorter than a fixed window length. We elaborate on this in more detail in the performance analysis section (Section 5.3). An efficient method to update $W(k)$ is presented in the sequel.

5.1.3. *Adaptive Window Length*

Our general idea to update the sliding-window length was based on the time distance between consecutive detected peaks whose amplitudes correspond to movements. In particular, the approach for finding the adaptive $W(k)$ was as follows. First, we needed to find local extrema in

the signal $x(k)$. Based on our observations, the amplitudes of movements were always higher than any type of breathing amplitude (as can be seen in Figure 4.1); therefore, extrema with low amplitudes were discarded. We considered the last two digits of the height of each bed occupant in cm as a bound (e.g., 70 for a 170 cm height). However, we may face some limitations in our decision. For example, if the bed occupant is an infant with a height less than a meter, this bound would not be applicable. Unfortunately, there was not a big variation of age ranges available for our data collection to see how this can affect the movement detection algorithm, but it can be considered as a potential future work.The detected extrema whose amplitudes were lower than this bound were disregarded. Moreover, for typical movements, a movement interval has at most three zero-crossings, and consecutive movements may not happen in less than 2 seconds. Therefore, if adjacent extrema happened in less than 20 samples (2 seconds) or if the number of zero-crossings was less than three, it was assumed that they both belonged to a single movement and only one of them was kept. Then, the new extremum was compared with the last kept extremum and we checked the two criteria again to decide whether or not it should be kept. The output of this stage was a set of time indices $i_1, i_2, ..., i_Z$ corresponding to the local extrema of $x(k)$. We started by initializing $W(k) = W_{\max}$, with a value of $W_{\max}$ set to 300. An adaptive window-length rule was proposed as follows, where $W(k)$ was updated at time indices $i_2, i_3, ..., i_Z$:

$$W(i_k) = \min\left(i_k - i_{k-1}, W_{\max}\right) \tag{5.3}$$

The updated window length was then kept unchanged until time i_{k+1}, when it was updated again using (5.3).

In the following, we present our movement detection scheme. The detection was declared by a movement indicator signal $I(k)$ which takes values from $\{0,1\}$. A given time k was declared within a movement interval if and only if $I(k)=1$.

5.1.4. *Onset Detection*

Our proposed scheme used the same movement onset detection method proposed in [1], where a control limit based on our proposed moving average and moving variance was used. An upper control limit (UCL) and a lower control limit (LCL) signal were constructed as follows:

$$\begin{aligned} UCL(k) &= \mu_x(k) + \kappa\sqrt{\sigma_x^2(k)} \\ LCL(k) &= \mu_x(k) - \kappa\sqrt{\sigma_x^2(k)} \end{aligned} \tag{5.4}$$

where κ is a fixed design parameter (with value to be determined later). If any two consecutive samples fell either above the upper limit or below the lower limit, we detected a movement onset time. Specifically, if

$x(k) > UCL(k)$ and $x(k+1) > UCL(k+1)$,

or

$x(k) < LCL(k)$ and $x(k+1) < LCL(k+1)$,

then a movement onset was detected.

5.1.5. *Offset Time Detection*

Once a movement onset was identified at time k, our scheme declared that the subsequent times were within the movement interval, until a movement offset condition was met. We used the following movement offset condition. At any time $k' \geq k$ for which all of the following three conditions were met, we detected a movement offset if

$dUCL(k') < \alpha$,

and

$dUCL(k'+1) < \alpha$, (5.5)

and

$dUCL(k'+2) < \alpha$

where $dUCL(k) = UCL(k) - UCL(k-1)$ shows the change in the upper control limit from time $k-1$ to time k. α is a design parameter which must be chosen properly to adjust the average offset delay. In Section 5.2 we investigated its effect on the performance of the proposed scheme.

5.1.6. *Postprocessing*

After the movement indicator signal $I(k)$ was found, we performed post processing according to the bed-occupant's physical attributes such as height and weight. Unlike the previous work in [1], we aimed to prevent our scheme from wrongly detecting different arbitrary sleep patterns as movement. For example, we found that deep breathing was more likely to be detected as movement. Since deep breathing increases signal variation, it is more prone to fall outside the control limits. We noticed that the signal amplitude during different sleep patterns and different actions varied from person to person. So we proposed to set a person-dependent parameter to allow reversing the false positive movement detections made from $I(k)$. At all k for which $I(k) = 1$, if $\sigma^2_x(k) < \rho$, we changed $I(k)$ to zero. We proposed the following formula for ρ:

$\rho = 3 \times \left(\text{weight (kg)} + \text{last two digits of height (cm)} \right)$ (5.6).

5.2. *Experimental Results and Performance Analysis*

We begin by providing an example of how our peak detection process works. A measured signal $x(k)$ from one of the 20-minutes long recording data is depicted in Figure 5.1.

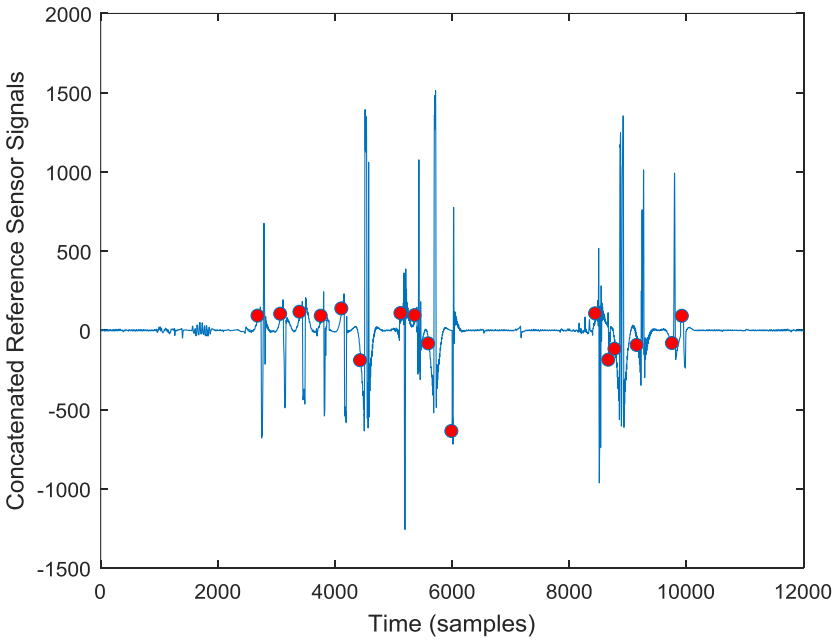

Figure 5.1. An example of the peak detection process

As can be seen, all the 16 detected peaks correspond to the real 16 movements, which were perfectly detected. Low amplitude spikes in the signal indicate the times that a person changed his/her breathing pattern. Closely located peaks belong to consecutive movements which occurred less than 30 seconds from each other. In the following we investigate the performance of our proposed movement detection scheme for different experimental cases. Our experiments revealed that a suitable value for κ in (5.4) is 3.0, and for the rest of this chapter we considered this value for κ. Recall that our proposed offset detection was based on comparing the amount of decrease in the upper control limit signal for three consecutive samples with the pre-set threshold α. Different values of this parameter resulted in different endpoint time detections. Generally

speaking, the larger values of α will result in early offset detection as the conditions in (5.5) are satisfied easily. On the other hand, as the value of α decreases, larger drops in the upper control limit are required. As a result, we will have later offset detections. Figure 5.2 shows the behavior of the average offset delay with respect to α. We applied the proposed method to the first set of 20-minutes long data collected from the five participants mentioned in Section 4.2.1.

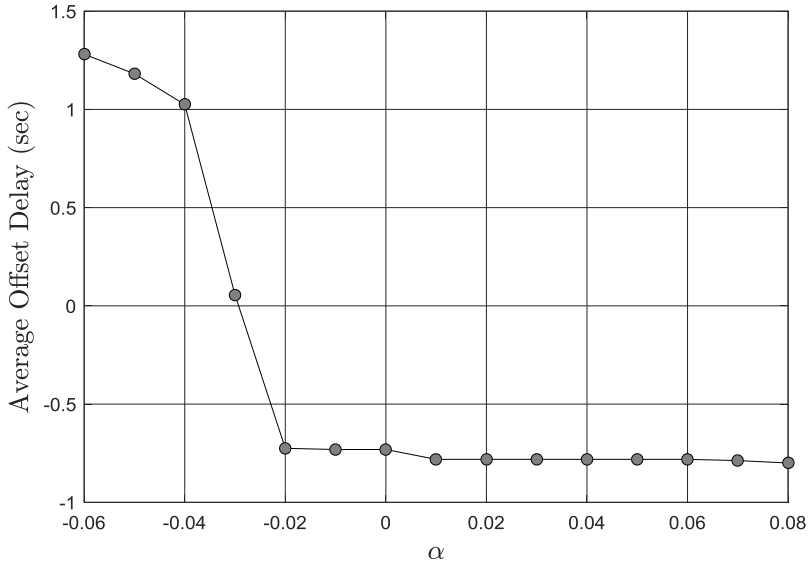

Figure 5.2. The effect of the threshold α on the average offset delay

The vertical axis in Figure 5.2 shows the average offset delay for different values of α averaged over all the participants. As can be seen, a small value of α results in large offset delays. For example, for $\alpha = -0.06$, the average offset delay is around 1.3 seconds. That is, we declare that a detected movement has ended on average 1.3 second after it actually ended. As α increases, the average delay decreases to a point where it becomes zero. After this point increasing α further will result in a negative delay, which means we declare that a detected movement has ended before it actually did. For example, with $\alpha = 0$, we declare that the movement ended on average 731 ms before it actually ended. From Figure 5.2, we found that the best value for α to minimize the

absolute value of the delay was around $\alpha = -0.029$. We used this value of α for the remainder of this chapter.

Figure 5.3 depicts the movement onset and offset detection results for a participant laid on a bed for 20 minutes. For better visualization, we only included the results for a short period of time. The blue curve shows the time intervals in which the actual movement has occurred (with 0.0 for no movement, 1.0 for movement, multiplied by -1000.0 in Figure 5.3 for better visualization). The red curve is the resulting movement indicator signal $I(k)$ (multiplied by +1000.0), and the grey curve shows the concatenated reference sensor signal.

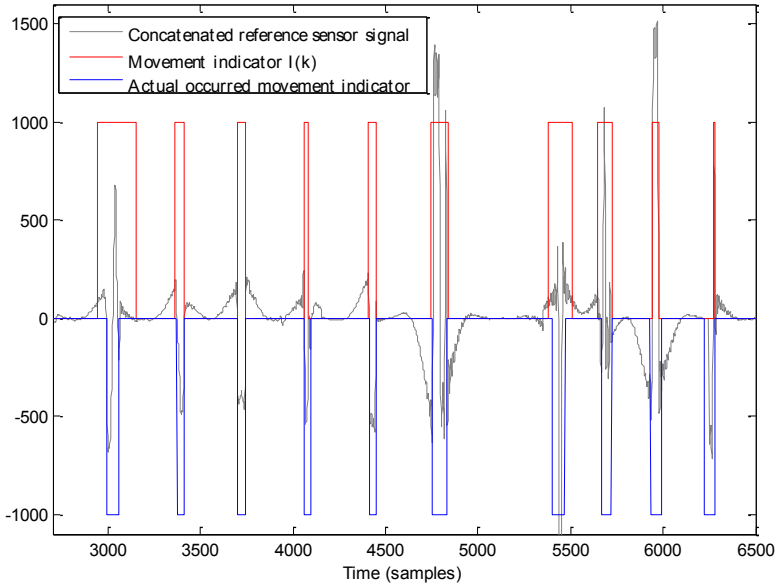

Figure 5.3. A sample movement detection result

We also show the results obtained from the nocturnal data (volunteers #6 and #7) in Figure 5.4. The black curve is the concatenated reference signal and the red curve (with diamond signs) is the movement indicator signal multiplied by 1000.

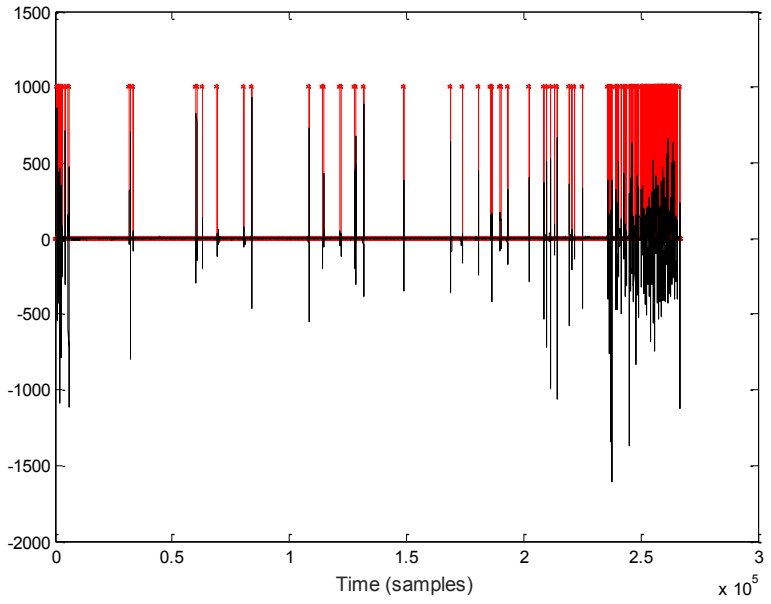

a) Nocturnal data in female subject (Volunteer #6)

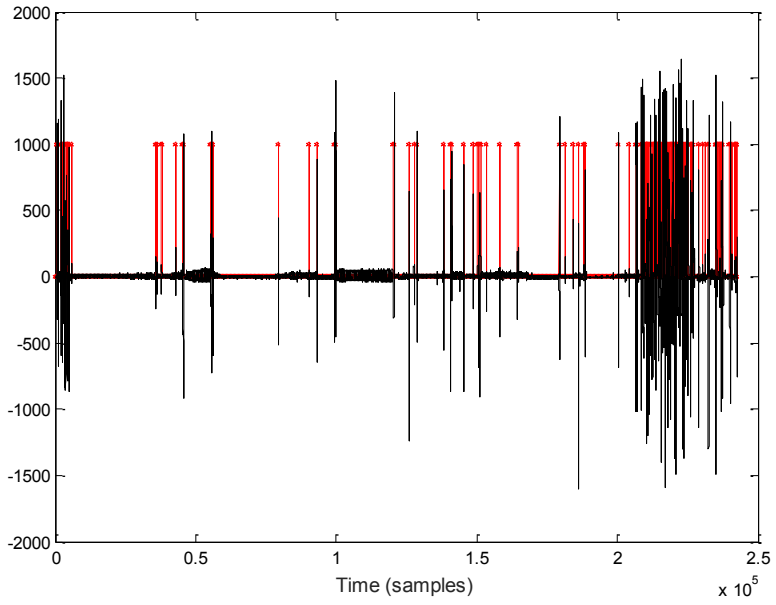

b) Nocturnal data in male subject (Volunteer #7)

Figure 5.4. The movement detection results for nocturnal data

The proposed method resulted in low numbers of false-negative events and no false detection events. A false-positive is an event when a movement is detected while no movement has actually

occurred, while a false-negative is an event where a method fails to identify an occurred movement. Based on our observation of signals before and after the post-processing step, we found that false-negative events in our data occurred after the post-processing stage. In those few undetected real movements (2 for male subjects and 3 for female subjects), the moving variance signal was slightly below the threshold ρ. Therefore, in the post-processing stage, while comparing the moving variance signal with a threshold, the method had wrongly removed those occurrences. There is another case that could result in a false-negative event, where the peak detection process could not detect all peaks related to movements, resulting in not updating the window length for the undetected peaks. In this case, if undetected peaks have a shorter time distance to the prior detected peak compared to the previous computed distance, we may get a false-negative event for a peak. While if the undetected peak does not have a shorter distance to the previous detected peak compared to the previous computed distance, we may still be able to detect the movement with the un-updated window length. We did not obtain any false detection events in the nocturnal data of the two subjects for which such data was available.

A performance analysis of our proposed method and a comparison with previous work on movement detection with pressure sensor arrays was done in terms of average movement onset delay, average movement offset delay, as well as the number of false detections and false-negative events. The average onset/offset delays are defined as the average time difference between a true movement onset/offset and the detected one. Table 5.1 compares the performance of the proposed method with the method from [1].

Table 5.1. Comparison of the proposed method and the method from [1].

Gender	Number of Movements	Average onset Delay (sec)	Average offset Delay (sec)	False-positives	False-negatives
M, proposed	105	-0.97	1.76	0	2
M, using [1]	105	-1.39	8.14	7	9
F, proposed	137	-0.96	1.32	0	3
F, using [1]	137	-1.67	9.21	9	12

As can be seen from this table, our proposed method outperforms the method in [1] in terms of all four performance metrics. Over the limited number of movements that we processed in the recordings (242 in total), our proposed method led to a low number of false-negatives and zero false-positive events. Also, with our proposed method the average offset delay was significantly lower, as a result of adjusting the required amount of decrease in the UCL signal for the three consecutive samples. This was achieved by choosing the optimum value of $\alpha = -0.029$ to minimize the average offset delay. However, we should note that the improvement in the performance over the method from [1] comes at the price of increasing the processing complexity, mainly due to the adaptive window length and the peak detection procedure.

5.3. *Concluding Remarks*

A new method to perform in-bed movement detection using unobtrusive pressure-sensor array was proposed. Using an adaptive window-length to calculate a moving average and a moving variance based on the local extrema of the sensor signal, a method resulting in very low false-negative events was developed. Also, by performing post processing to take into account the

physical attributes of the participant, low false-positive rates were achieved. By allowing the derivative of an upper control limit to be compared with a threshold, we adjusted the average offset detection delay to be as low as 1.32 second. The proposed method was capable of detecting different movement types, including slight and gross movements.

Chapter 6. SNR-Max Signal Fusion Method for Respiratory Rate Estimation

In this chapter, a new signal fusion method is first presented, which was published in [3]. The performance of this method is also analyzed by comparing to other fusion methods. Moreover, breathing rate estimation during movement as examined in [32] is investigated and new results are presented, obtained by applying the new movement detection algorithm (previous chapter and [2]) and a small modification on the limitation in the sensor signal selection method in [32]. These new findings appear in [4].

There exist many ways for breathing rate monitoring. The authors in [48, 49] presented non-contact video-based breathing rate monitoring methods. However, people are often reluctant to undergo video capturing since it does not preserve their privacy. Prior to their work, a Harmonic Path (HAPA) algorithm was also suggested in order to monitor breathing rate and heart rate by non-contact Impulse Radio Ultrawideband (IR–UWB) radar [50]. In general, the unobtrusive and automated nature of monitoring has a high influence on patients' acceptance of home-based technology. Therefore, we aimed to carry out an investigation on the extraction of breathing signal and breathing rate using unobtrusive pressure sensitive sensor arrays. These can be placed on top or below a mattress to measure values proportional to the respiratory pressure exerted on it. Multiple sensors can pick up the bed occupant's respiratory efforts and the most representative sensors can be selected. Previous research used the sum of all sensor signals as a breathing signal estimate [33], and we proposed in [3] a breathing signal estimate extracted by combining sensor signals through an SNR-maximizing method based on a beam-former derivation, which we refer to as the SNR-max method in this thesis. More processing could be added to produce pressure

images in order to localize the torso area of the bed-occupant [51]. This would lead to a better selection of the sensors with breathing information; however, it would also bring the complexity and cost up as the pressure image construction and analysis would have to be included in the rate estimation process.

A comparison among some methods such as radars, cameras and Ballistocardiogram has been described in [52] with special emphasis for the measurement of physiological information in preterm infants. This comparison was performed in terms of the quality provided by different measurement methods in capturing different signals (signals with mechanical root such as heart rate and breathing rate, signals with electrical root such as Electroencephalography and Electrocardiography, and behavioral signals such as body movement). Movement artifacts lead to devastating physiological characteristics in the signals extracted by several measurement methods. Therefore, the authors in [52] concluded that camera monitoring is the optimal solution which can provide measurement for the three aforementioned types of signals. However, camera monitoring has its own disadvantages. For instance, it leads to loss of privacy which makes people reluctant to share their daily activities with interpreters, researchers or clinicians, even if it can provide health benefits. Moreover, if the camera is blocked or repositioned somehow by a caregiver or a staff, sleep monitoring will be stopped.

Pressure sensitive sensors are highly pliable. This sensitivity enables users to put the pressure sensor arrays beneath the mattress with no discomfort, obtrusiveness, or impact on the user's privacy and sleep. Therefore, we used this measurement method in our work. The method presented in this paper allows to estimate the breathing rate with pressure sensitive sensor arrays. The significance of our method is that it is capable to estimate breathing rate in all periods of times, even in movement occurrences, with a better reliability compared to prior work [32].

Movement is a corruptive factor which can interfere with breathing signal estimation. It also affects the sensor signal selection, as the representative sensors that are picked might be the ones most affected by movements. Therefore, we first identified movements by a new movement detection algorithm as in [2] and then applied a method as in [32] to minimize its effects.

6.1. *SNR-Max Beam-Former*

A brief explanation of combining sensor signals according to the theory of SNR-maximizing beam-former (SNR-max) is presented in this section.

Based on Chapter 6 of [53], the goal of using this approach for combining signals is to maximize the SNR of the combined signal. For single-tap per sensor signal solutions as the one proposed here, it is explained in [53] that except for a scale factor which does not affect the output combined signal SNR, the solution (weights, coefficients) of the SNR-max beam-former is the same as for a Minimum Variance Distortion-less Response (MVDR) beam-former. The MVDR beam-former minimizes the noise level in the output combined signal without distorting the desired useful signal in the output. As the MVDR formulation is widely found in beamforming designs, the SNR-max beam-former solution is derived below using the MVDR solution.

The system process is illustrated in Figure 6.1 to present a better view of implementing a combiner fusing the sensor signals associated with each channel.

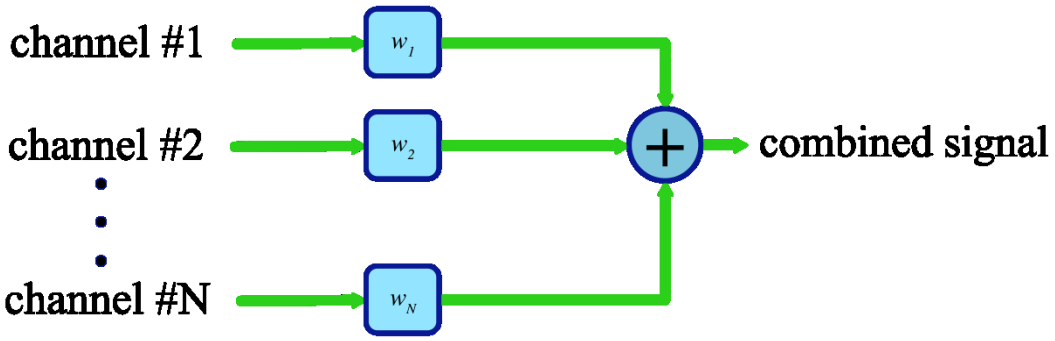

Figure 6.1. Combination process

The $W_n = [w_1\ w_2 \cdots$ tap coefficients are the weighting factor of each sensor signal. The optimal W_n values for segment *n* are computed based on an auto-correlation matrix of the noisy input signals $R_{CC,\mathrm{n}}$ and a "steering vector" D_n:

$$W_n = \frac{\left(R_{CC,\mathrm{n}} + \mu I\right)^{-1} D_n}{D_n{}^H \left(R_{CC,\mathrm{n}} + \mu I\right)^{-1} D_n} \tag{6.1}$$

where D_n consists of the response between the desired (useful breathing) signal in the reference sensor and all other desired signals in the other sensors, and μ is a regularization parameter to deal with ill-conditioned problems.

As the output signal SNR cannot be affected by a constant scaling factor applied to D_n, any normalization can be performed on D_n. For example, the D_n vector components can be computed from the ratio of cross-covariance between reference signal components and all other sensor signals, over the auto-covariance of the reference signal, which then corresponds to the one-coefficient impulse response between the reference sensor and the other sensors:

$$D_n = \begin{bmatrix} \frac{\sum_{i=1}^{M}(C_{n,1}[\mathrm{i}]-\bar{C}_{n,1})(C_{n,r}[\mathrm{i}]-\bar{C}_{n,r})}{\sum_{i=1}^{M}(C_{n,r}[i]-\bar{C}_{n,r})^2} \\ \frac{\sum_{i=1}^{M}(C_{n,2}[\mathrm{i}]-\bar{C}_{n,2})(C_{n,r}[\mathrm{i}]-\bar{C}_{n,r})}{\sum_{i=1}^{M}(C_{n,r}[\mathrm{i}]-\bar{C}_{n,r})^2} \\ \vdots \\ \frac{\sum_{i=1}^{M}(C_{n,N}[i]-\bar{C}_{n,N})(C_{n,r}[n]-\bar{C}_{n,r})}{\sum_{i=1}^{M}(C_{n,r}[\mathrm{i}]-\bar{C}_{n,r})^2} \end{bmatrix} \tag{6.2}$$

But the denominators (normalization) in the above equation are not required and can be removed to reduce complexity. Moreover, since we are working with bandpass filtered signals, it is unnecessary to remove the means $\bar{C}_{n,1}, \bar{C}_{n,2}, \cdots$ in the above equation. Note that the above equation is only an approximation, as ideally it should be computed using only the useful desired breathing components in the different sensors. But in our application the equation is computed using the total bandpass filtered sensor signals (including both the useful signal and noise).

The global auto-correlation matrix $R_{CC,\mathrm{n}}$ for segment *n* is normally calculated as follows:

$$R_{CC,\mathrm{n}} = \frac{1}{M}\sum_{i=1}^{M}\left(C_n[\mathrm{i}]C_n[\mathrm{i}]^T\right) \tag{6.3}$$

with $C_n[\mathrm{i}] = \left[C_{n,1}[\mathrm{i}]\, C_{n,2}[\mathrm{i}] \cdots \right]^T$. When the value of the D_n vector is not accurately known, using the noisy signals correlation matrix $R_{CC,\mathrm{n}}$ instead of a noise-only correlation matrix in equation 6.1 can lead to a significant performance degradation of the beam-former and some signal attenuation or distortion in the useful output combined signal. However, this is of no concern if we

assume that the noise is spatially uncorrelated between sensors and that it has the same variance in each sensor, such that $R_{CC,\mathrm{n}}$ becomes a scaled identity matrix. In this case, up to a scalar term, equation (6.1) becomes simply:

$$W_n = D_n ,$$

i.e., it has the form of a "matched filter" and there is actually no need for computing $R_{CC,\mathrm{n}}$. The final combined output of the beam-former is calculated as follows:

$$y_n[\mathrm{i}] = W_n^T C_n[\mathrm{i}] \qquad (6.4).$$

In the rest of this chapter, the performance of this method is examined in respiratory signal extraction by comparing this method with other state-of-art breathing signal fusion techniques. Moreover, an improved sensor selection method for signal combining is presented to obtain higher reliability in breathing rate estimation.

In Chapter 8, the SNR-max beam-former combining method will be used to extract breathing signal from long-term data, in order to see breathing rate variability over time.

6.2. *Methods and Materials*

Figure 6.2 shows the estimation processing system used in this chapter in order to estimate breathing rate. Breathing signals are highly disrupted by movements. Therefore, movements should be detected and suppressed before using the rate estimation method. We aimed to select the sensors representing respiratory efforts based on both variance and spectral flatness ratio of the sensor signals, rather than only considering the variance calculation. Moreover, the movements were suppressed with higher accuracy using a recent algorithm of movement detection [1], which outperforms previous methods of movement detection. We used the same reliability metric

methodology as those reported in [32] and [54] in the data fusion and final breathing rate decision reliability.

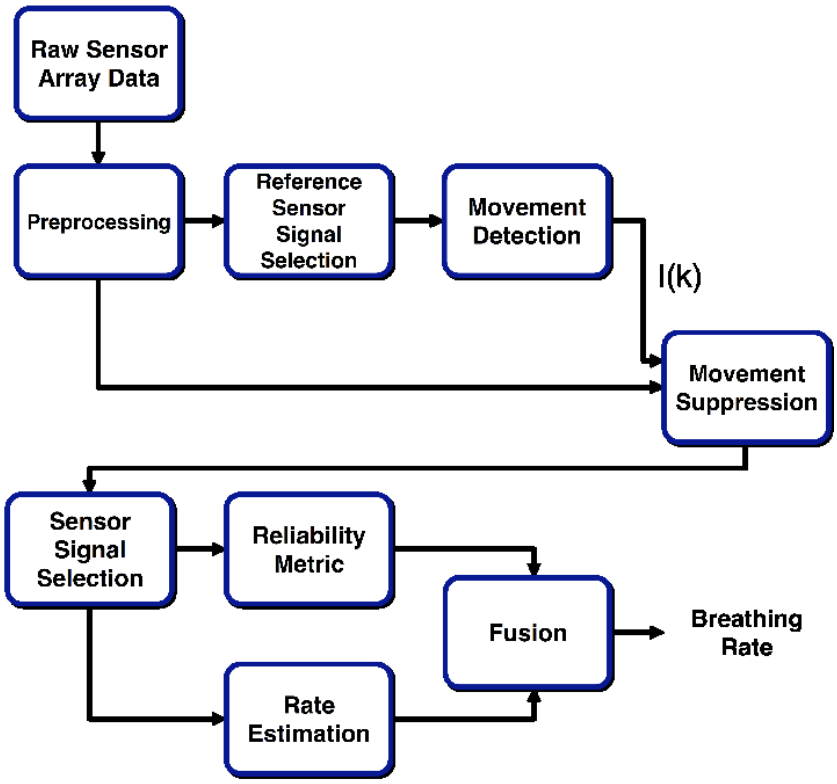

Figure 6.2. Block diagram of rate estimation process

We used the proposed algorithm of movement detection with adaptive window length moving variance and moving average presented in Chapter 5. This method finds a movement indicator signal, $I(k)$ as follows:

$$I(k) = \begin{cases} 1 & \text{if movement detected at sample k} \\ 0 & \text{otherwise} \end{cases} \tag{6.5}$$

Later on, we used this $I(k)$ indicator in the rate estimation process to diminish the effect of movements in sensor signals.

6.2.1. *Preprocessing*

The same segmentation and filtering processes described in Section 5.1.1 were used prior to the rate estimation algorithm.

6.2.2. *Sensor Signal Selection*

Before applying the sensor selection method, we needed to minimize the effect of movement in sensor signals. Therefore, we used the same movement suppression method proposed in [2], where movement samples were substituted by zeros and the other samples were processed by removing their mean, leading to:

$$s_{(i,n)} = \begin{cases} z_{(i,n)_{I=0}} - E\left[z_{(i,n)_{I=0}} \right] & \text{for } I = 0 \\ 0 & \text{for } I = 1 \end{cases} \tag{6.6}$$

where $s_{(i,n)}$ are the samples of the n^{th} sensor signal in the i^{th} segment after movement suppression and $z_{(i,n)_{I=0}}$ are the samples of the n^{th} sensor signal in the i^{th} segment before movement suppression.

There are several ways to perform signal selection for respiratory rate estimation. We can select only one sensor signal based on the maximum average power as we did in [2] for movement detection purpose. We can also pick several sensor signals and fuse the results of these signals to extract a single output, using combining methods which can produce a high correlation with a gold standard method in data free of movement [3]. Previous work on respiratory rate estimation during movement [32] also suggested selecting only the sensor signals with a variance above the equipment's noise power.

Our general idea for finding signals of interest was to select sensor signals based on two parameters: variance and Spectral Flatness Measure (SFM), which is also called a tonality factor. Sensors exhibiting variance and SFM within our margin were kept and the rest was discarded. Afterwards, we fused the results obtained from all the remaining sensor signals.

SFM is the ratio of the geometric mean of the signal power spectral density to the average of the signal power spectral density [55]. It produces a value between 0 and 1, where the highest value shows that a spectrum is flat. SFM is constructed as follows:

$$SFM = \frac{\left(\prod_{k=0}^{K-1} x_k^2\right)^{\frac{1}{K}}}{\frac{1}{K}\sum_{k=0}^{K-1} x_k^2} \tag{6.7}$$

where x_k represents the magnitude of bin number k in a discrete Fourier transform.

We set a threshold for the variance and the SFM, to avoid choosing sensor signals swamped by either movements or noise rather than respiratory efforts. We used the same threshold on variance as we used in the post-processing step in [2], so that signals with a variance above this threshold and below the noise threshold were discarded. The threshold for SFM was obtained by trial and error varied among different participants.

6.2.3. *Breathing Rate Estimation*

Researchers have used different methods to determine breathing rate from respiratory signals [56, 57]. Since the autocorrelation approach has been found to be more efficient in estimating the breathing rate [32], we applied this in order to obtain the breathing rate from the remaining signals. Our proposed scheme used the same reliability metric, reliability estimate and data fusion proposed in [32]. The reliability metric is based on a weighting measure obtained from the autocorrelation

function of the remaining sensor signals, multiplied by the percentage of samples (in each segment) that do not contain movements.

6.3. *Experimental Results and Performance Analysis*

We evaluated the performance of our method by comparing it with the previous work in [32]. To this end, the nocturnal data that were collected from a female and a male described in Section 0 were used. Figure 6.3 and Figure 6.4 show the respiratory results obtained overnight from both participants. Results were calculated with three different methods: 1) using SNR-max combined signal [3] with movement suppression, 2) with the previous approach in [32] but including the new movement detection algorithm, and 3) with our new proposed enhanced method using the tonality factor and upper variance limit.

Despite having more than 50% of data corrupted by movements, enhancing signal quality using the SNR-max combining method and suppressing movements with the new movement detection algorithm, we achieved more accurate estimates resulting in 18.15 and 13.67 mean breathing rate per minute and 12.18, 9.93 variance for female and male subjects, respectively. This was to be compared with 24.08 and 18.29 mean breathing rate values with 96.45, 83.70 variance, when using the sum of all sensor signals with no movement suppression and with the “no depletion of data” fusion technique, respectively.

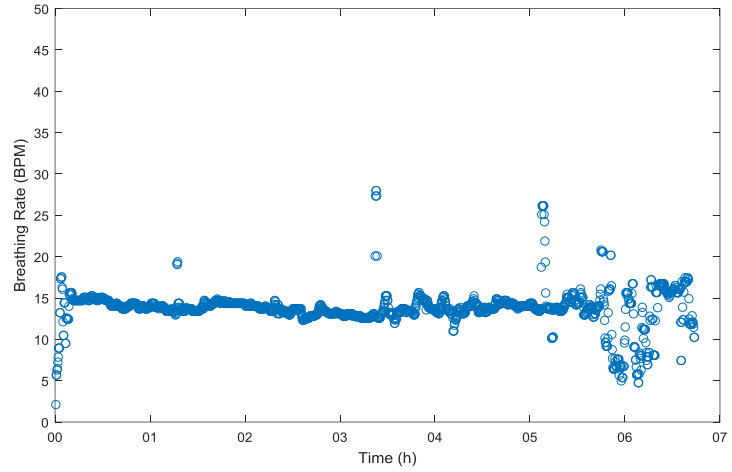

a) With movement suppression on SNR-max combined signal.

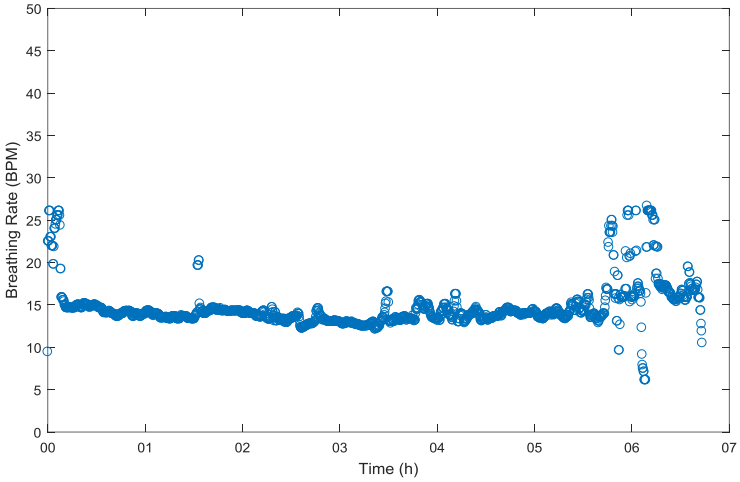

b) With movement suppression on variance-dependent data fusion method

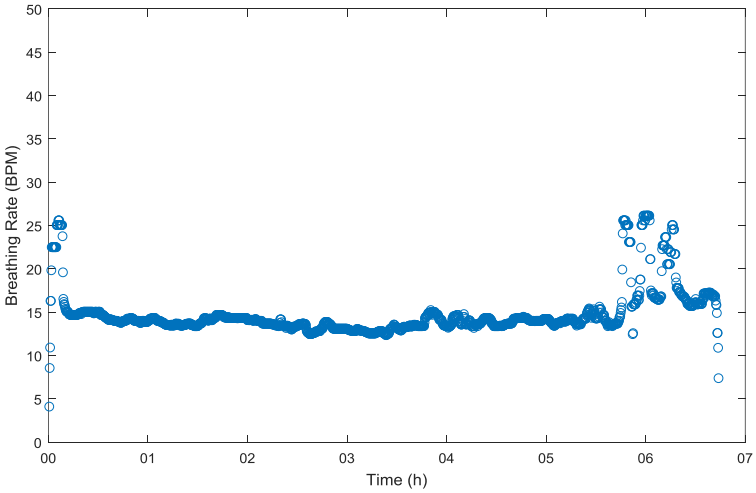

c) With movement suppression on variance-tonality dependent data fusion method

Figure 6.3. Nocturnal respiratory rate results of male subject

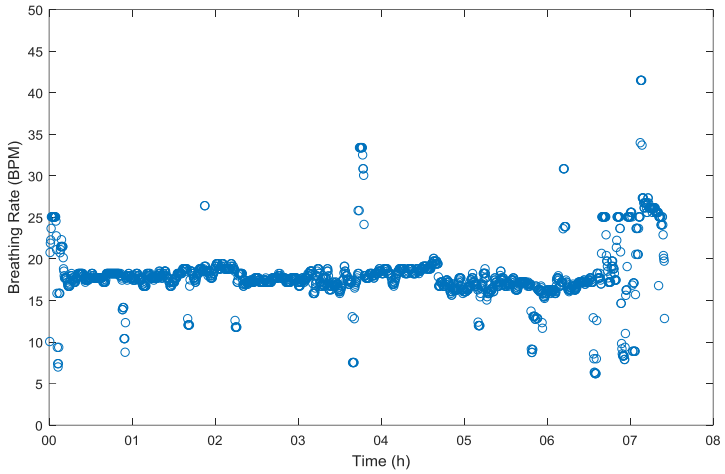

a) With movement suppression on SNR-max combined signal.

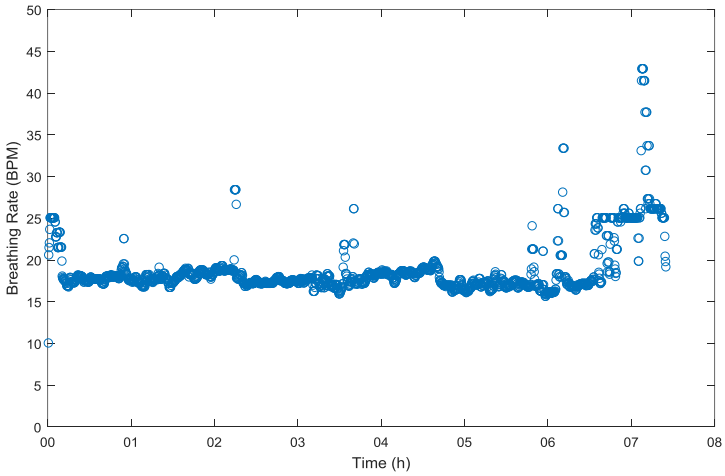

b) With movement suppression on variance dependent data fusion method

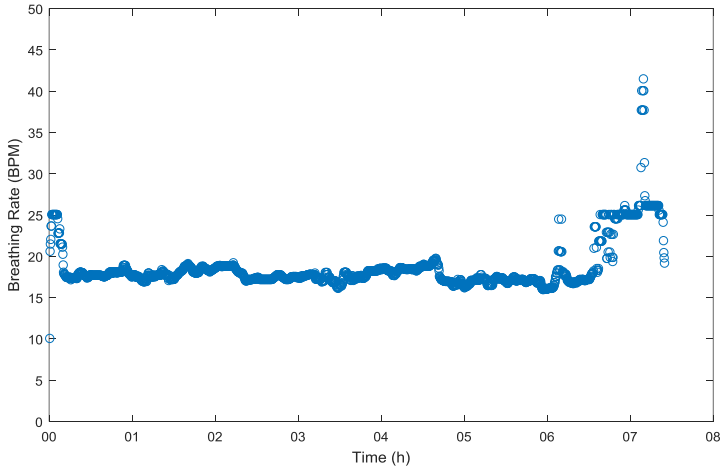

c) With movement suppression on variance-tonality dependent data fusion method

Figure 6.4. Nocturnal respiratory rate results of female subject

The movement suppressing and signal quality enhancing methods improved the performance and reduced the variance of the estimates. Nevertheless, some incorrect estimates was still observed, especially at the beginning of data collection while a person was trying to fall asleep and moved a lot in the bed, and also near the end of data collection, when a person woke up and started moving and rolling for a while in the bed. In general, breathing rate is expected to be higher and quite variable when a subject is awake compared to the deep sleep state. The SNR-max combined signal was found to be the best method overall for sensor signal combining resulting in the highest Pearson Correlation Coefficient (PCC) with the respi-band signal, compared to other data fusion methods. Some other possible metrics could have been considered to examine the signal quality captured from pressure sensor arrays such as the SNR; however we decided to determine the similarities between the captured signal from sensor arrays and the gold standard by PCC as in previous work. Results are shown in Table 6.1. Comparison was made with: (1) choosing only a reference sensor based on maximum average power [2], (2) sum of polarity and delay adjusted signals [42], (3) sum of polarity-corrected signals [42], (4) Maximal ratio combining method [44] and (5) SNR-max method [3]. Figure 6.5 shows a typical SNR-max combined signal obtained from a pressure sensor array for the first male participant in Table 6.1. The corresponding breathing signal measured by a respi-band is also plotted in this figure (it was synchronized with the signal obtained from the pressure sensor array prior to demonstration, including sample rate conversion and start time alignment).

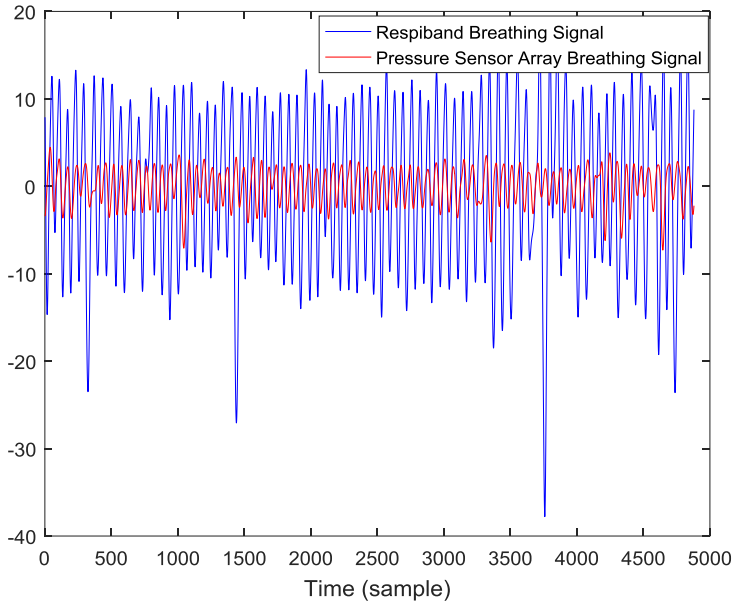

Figure 6.5. Breathing signal measurement by pressure sensor array and respiratory band

The breathing rate estimation method in [32] was also implemented for comparison. This method was compared with the proposed sensor selection method in Table 6.2. With our improved movement detection algorithm, we used a more restricted sensor signal selection method by setting two conditions compared to only one in [32]. Therefore, we expected to observe a higher performance in the enhanced breathing signal extraction method, leading to higher reliability estimate compared to the method used in [32].

Table 6.1. Pearson Correlation Coefficient for different combining methods

Gender	PCC (1)	PCC (2)	PCC (3)	PCC (4)	PCC (5)
Female 1	0.62	0.76	**0.82**	0.77	**0.81**
Male 1	0.87	**0.90**	**0.90**	0.85	**0.91**
Female 2	0.56	0.41	0.49	0.55	**0.64**
Male 2	0.47	**0.52**	**0.52**	0.50	**0.54**
Female 3	**0.75**	0.71	0.63	0.69	**0.77**

Table 6.2. Results from the different methods

Gender	Mean Reliability Metric	Estimate Reliability > 50	Estimate Reliability < 50	Percent with Movements	Percent Reliable	Mean Rate (BPM)	Variance
F, proposed	**72.69**	**1362**	**417**	55.08%	**76.55%**	18.58	**8.42**
F, using [32]	68.71	1335	444	55.08%	75.04%	18.76	11.26
M, proposed	**64.68**	**1216**	**399**	52.38%	**75.29%**	14.72	**7.21**
M, using [32]	61.41	1186	429	52.38%	73.43%	15.16	9.47

As can be seen from Table 6.2, with the new approach we reached a higher averaged reliability metric. Also, if we consider reliable results as those with a reliability estimate exceeding 50, we notice an improvement in the total percentage of reliable values as well.

6.4. *Concluding Remarks*

An improved method was presented in this chapter to perform breathing rate estimation with bed occupancy sensor arrays. We used recent work on movement detection combined with variance and SFM as indicators to select the most appropriate sensor signals. This new method led to a higher number of reliable estimates and improved mean reliability metric for movement-corrupted data. Moreover, the SNR-max method was also found to have better overall signal quality compared to other data fusion techniques. However, for a better comparison, a gold standard must be used which is not sensitive to movements in order to capture real breathing estimates during movement occurrences. This can be used to compare the breathing estimates obtained by different methods mentioned in this chapter with the real breathing estimates. That way, the best method can be chosen with higher assurance. This was a limitation in this work, which can be investigated in future work.

Chapter 7. Detection of Occupied Times with Available Respiratory Information

The main reason of conducting bed occupancy detection in this thesis was to enhance processing efficiency of the big data, since for a long-term monitoring practice most of the data are not relevant as no one occupies the bed for the whole day. Hence, in order to eliminate the irrelevant data and increase the processing efficiency, the bed occupancy needs to be determined accurately.

The bed occupancy monitoring method presented in Section 3.3.2 provides reasonably accurate results with a short processing time for bed-based pressure sensor arrays [46]. However, as the threshold selection in this method depends on anthropometric information of participants and there was no prior anthropometric information available in our studies, some modifications were required to be applied on this method. Moreover, in order to estimate reliably the respiratory rate, sensors must sense slight respiratory movements for various human gestures in the bed, which is not feasible in real life situations. Therefore, a method needs to be developed to detect not only the occupancy time but also the available respiratory information. Both of these two methods were compared to decide which approach provides reasonably accurate results with acceptable processing time.

7.1. *Methods and Materials*

In Section 7.1.1, the threshold-based occupancy detection method (i.e., previous method) is described in detail, followed by a presentation of an enhanced method (Section 7.1.2) in order to detect available respiratory information in the detected occupied times captured by the previous method. Both methods resulted in occupancy indicators, which are compared in Section 7.2.

7.1.1. *Occupancy Indicator by Thresholding Method*

Raw sensory data obtained in Section 4.2.3 were first refined in order to only keep those related to occupied times. To do so, a method similar to the one introduced by Pouliot *et al.* was used [46]. No preprocessing step was needed in this stage. The threshold was applied on the single output obtained from the summation of all 72 raw sensor signals (denoted as Z). Using this approach, occupancy was determined when this signal exceeded a threshold defined by:

$$T = \beta + \tau \tag{7.1}$$

where β is the base value obtained by averaging Z over the period of 1-minute data collection when no one occupies the bed. To make τ independent from the person who is lying in the bed, τ was established based on using maximum and minimum value of Z during the entire time of data recording, respectively denoted by $Max(data)$ and $Min(data)$, such that

$$\tau = \frac{Max(data) - Min(data)}{n} \tag{7.2}$$

where n can be adjusted depending on the sensitivity required in an application. To avoid false detection of occupancy, a condition was stipulated where occupancy or non-occupancy less than 30 seconds were disallowed. Also, if the difference between $Max(data)$ and $Min(data)$ is insignificant, it means that no occupancy occurs during data collection time.

Several prototype algorithms were examined to come up with robust bed occupancy detection parameters which were compatible for all type of patients and mattresses.

Applying this threshold on the sum signal ($z(k)$) will result in an occupancy indicator, $I_{Occupancy}$, demonstrating occupied times versus non-occupied times:

$$\mathrm{I}_{Occupancy}(k) = \begin{cases} 1 & \text{if occupancy detected at sample k} \\ 0 & \text{otherwise} \end{cases} \tag{7.3}.$$

The occupied data obtained in this step were kept and the rest of data were discarded. On the remaining data, a post-processing step was carried out to accurately determine the occupied times where breathing information was available. The maximum distance among active sensors was used to detect the periods where breathing can be measured with the pressure sensor mats. The reason that we came up with utilizing the maximum distance is because respiratory information is known to be available when a person is lying in bed, and the maximum distance distinguishes the periods a person is lying in bed versus several other positions (sitting, reading, etc.).

7.1.2. *Occupancy Detection for Available Respiratory Information*

The steps to proceed with this method were as follows:

- Finding exact pattern of sensor placement on arrays
- Identifying the active sensors and discarding the rest
- Calculating distance between the active sensors
- Finding maximum distance in each sample (k)
- Selecting an appropriate margin to detect the availability of respiratory information

First, in order to find the maximum distance among active sensors, pressure distribution visualization was required. To do so, sensors were mapped to their original places on the sensor array. The black mat and three concatenated white mats (containing 72 sensors each) have different mapping positions (i.e., sensor placement). Sensor placement was identified as follows:

13	17	21	37	41	45	61	65	69
01	05	09	25	29	33	49	53	57
14	18	22	38	42	46	62	66	70
02	06	10	26	30	34	50	54	58
15	19	23	39	43	47	63	67	71
03	07	11	27	31	35	51	55	59
16	20	24	40	44	48	64	68	72
04	08	12	28	32	36	52	56	60

a) Three white mats

12	08	04	24	20	16	36	32	28
48	44	40	60	56	52	72	68	64
11	07	03	23	19	15	35	31	27
47	43	39	59	55	51	71	67	63
10	06	02	22	18	14	34	30	26
46	42	38	58	54	50	70	66	62
09	05	01	21	17	13	33	29	25
45	41	37	57	53	49	69	65	61

b) Black mat

Figure 7.1. Actual sensor placement in arrays

The active sensors were then defined as those with a pressure value which is at least 40% of the maximum possible value that the pressure sensor is able to exhibit. 40% is chosen in order to guard against small variations which appear in sensor signals due to small movements in bed not pertaining to bed occupancy. Afterwards, a distance calculation was conducted among the detected active sensors. Below, is an example of how distance is computed among sensor locations:

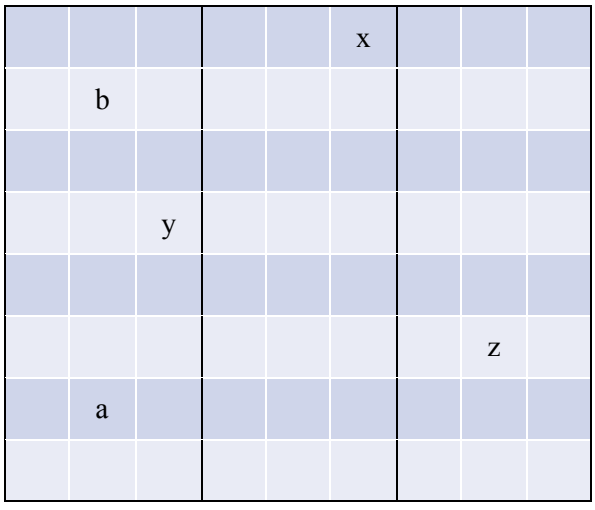

$$xy = \sqrt{3^2 + 3^2} = 4.2426$$
$$xz = \sqrt{2^2 + 5^2} = 5.3851$$
$$yz = \sqrt{5^2 + 2^2} = 5.3851$$
$$ax = \sqrt{4^2 + 6^2} = 7.2111$$
$$ay = \sqrt{1^2 + 3^2} = 3.1622$$
$$az = \sqrt{6^2 + 1^2} = 6.0827$$
$$ab = \sqrt{0^2 + 5^2} = 5$$
$$bx = \sqrt{4^2 + 1^2} = 4.1231$$
$$by = \sqrt{1^2 + 2^2} = 2.2360$$
$$bz = \sqrt{6^2 + 4^2} = 7.2111$$

Figure 7.2. An example of distance calculation in pressure sensor arrays

As the sensors were evenly spaced apart from each other, the Pythagora theorem could be used to determine the distance between sensors. Distances were calculated among all available pairs of active sensors and only the maximum distance value was kept at each sample (k) to be displayed later on. After finishing all calculations, a signal was constructed from the maximum distance obtained at each time sample (k). The most repetitive value (mode) in this signal will be chosen as the value demonstrating occupancy where breathing information exists. If the maximum distance value falls within a margin of 15% of the mode, it is considered as the time where respiratory information is available.

7.2. *Results*

In Figure 7.3 and Figure 7.4, typical occupancy detection results obtained from the two above-mentioned methods are plotted. As can be seen, the differences between these two methods are quite evident. The results shown in these two figures pertain to one of the participants in this experimentation. The actual start and end time of all events are also included in the figures. The orange curve shows the occupancy indicator which is magnified respectively by 50000 and 8 in Figure 7.3 and Figure 7.4, for better visualization. The sum of all sensor signals, shown in the figures, refers to signal Z over time. The deficiency of the method shown in Figure 7.3 comes from including periods of sitting, transitions, and particularly reading position as occupancy, which may lead to high number of inaccurate estimates in the breathing rate estimation process. Therefore, the maximum distance calculation algorithm was applied to remove these deficiencies as much as possible; the results of which are demonstrated in Figure 7.4.

In Figure 7.4, it is visible that the enhanced algorithm benefited the system by discarding several portions of data which were previously considered to be bed-occupied data in the absence of

respiratory information. Specifically, portion number 6 pertaining to reading status was eliminated from the occupancy indicator, which was completely included in the results of the previous occupancy indicator method (Figure 7.3).

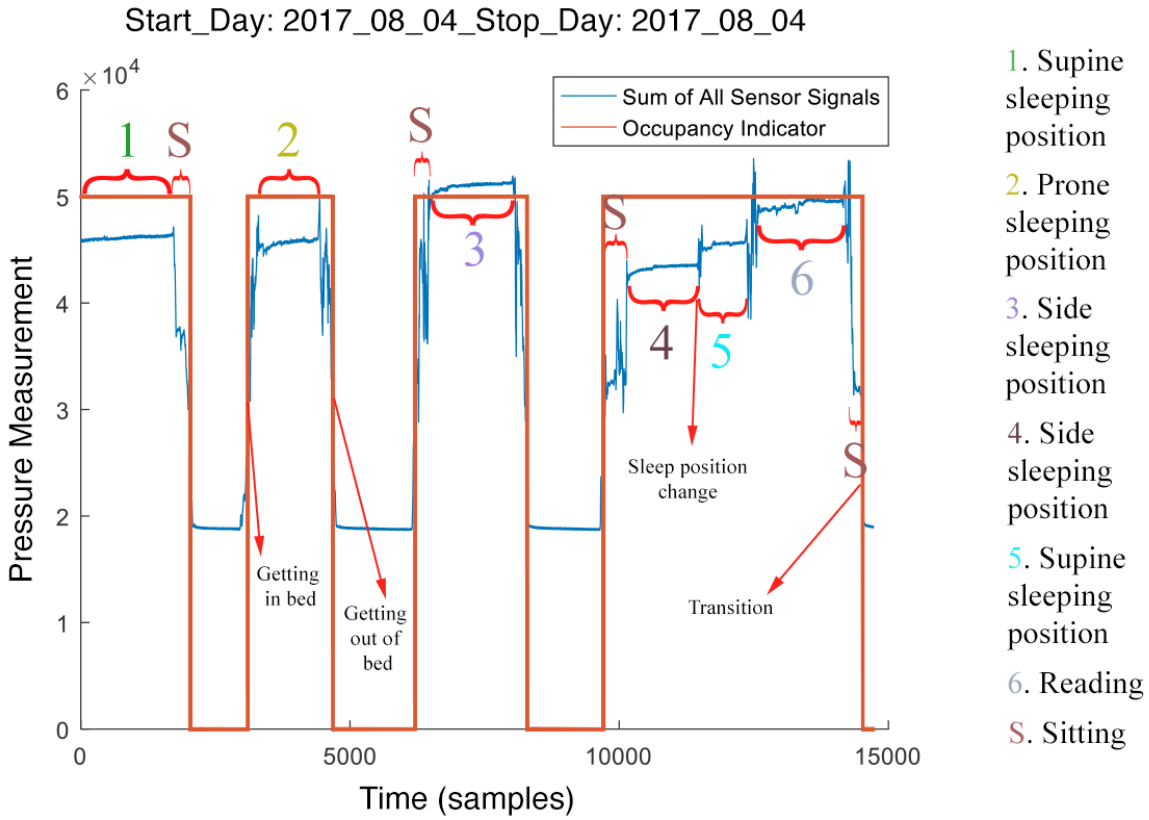

Figure 7.3. Occupancy detection from previous method on one participant

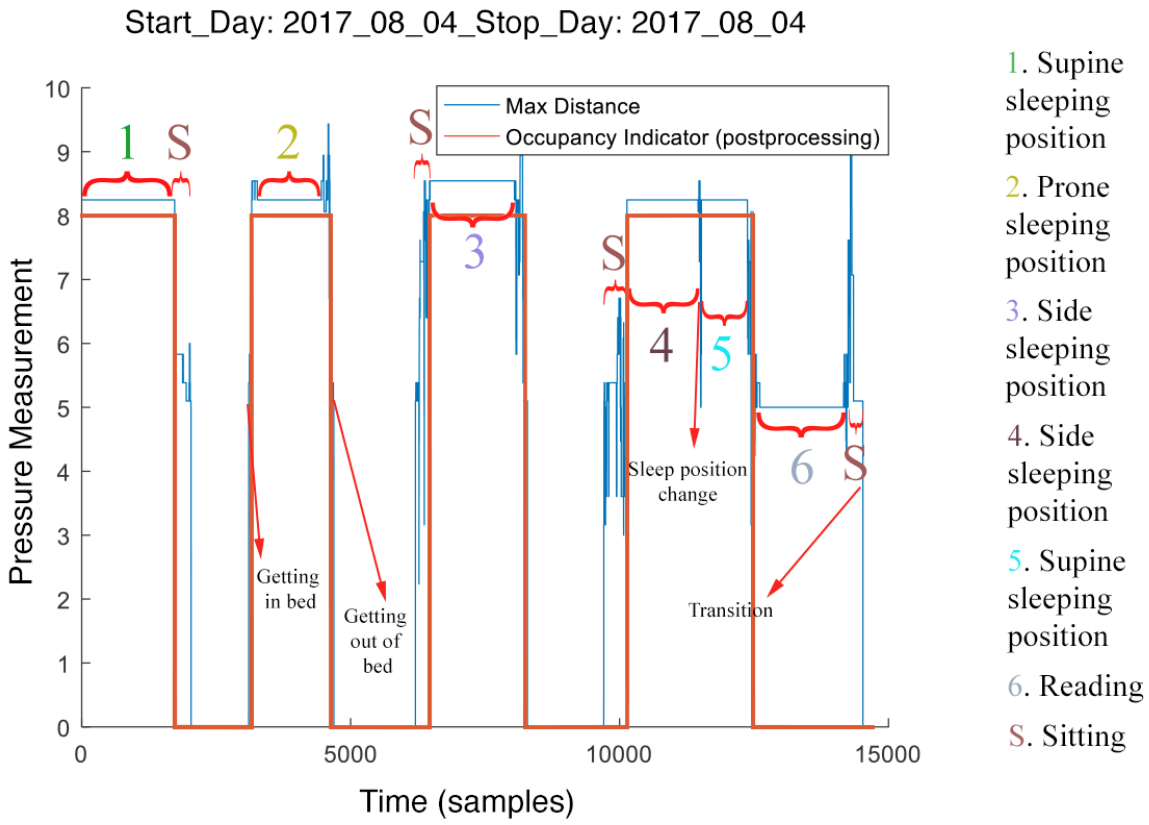

Figure 7.4. Occupancy detection from maximum distance method on the same participant

Table 7.1. Delays in start/end time of events for one participant

	Occ. Indicator (samples)	**Max. Dist. (samples)**	**Actual Time (sample)**	**Delay in Occ. Indicator (samples)**	**Delay in Max. Dist. (samples)**
Out 1	2033	1728	1728	305	0
In 2	3103	3160	3265	162	105
Out 2	4687	4613	4572	115	41
In 3	6204	6460	6467	263	7
Out 3	8286	8150	8070	216	80
In 4	9706	10136	10137	431	1
Out 4	14523	12376	12376	2147	0
			Average	519.85	33.42

Table 7.1 shows the delays obtained from both methods in detecting actual start/end time of events, excluding the ones which are not detected at all. “Actual time” refers to the time that a person starts the process of moving in order to get in/out the bed. “Occ.” refers to occupancy.

Actual times in Table 7.1 refer to the times when a person starts moving to get in/out of the bed. The delays come from the time difference between the time each method detected as in/out time and the actual in/out time. Delays are important as we were interested to remove the occupied times where respiratory information is not available (sitting and sit-to-stand transfers). Moreover, there is one position (reading), that the previous method was not able to detect in order to eliminate it (as it is also an occupied time where respiratory information is not available). Values in Table 7.1 are all written in samples. Repeating the experiment for all 5 participants with the same script led to minimizing the average delay to 1.92 s, corresponding to 38.4 samples in a 20 Hz bed mat array.

Despite the beneficial aspects of the maximum distance occupancy detection method, it is very costly and time-consuming, because complexity is greatly increased to build the detection system of this algorithm. Moreover, the processing time for occupancy detection was found to be high on our computer system with an Intel Core i7 2.93 GHz CPU, 8 GB RAM and Windows 7 professional SP1 64-bit, so maximum distance occupancy detection may not be practical in real-time processing.

For instance, the processing time required for performing each method in MATLAB are shown in Table 7.2 The data used for this purpose was selected from the big data. 5 days of recorded data for 5 different patients were randomly selected to compare the results in order to identify the most efficient method.

Table 7.2. Required processing time for performing the two methods

No.	Participant Num./ID	Samples Count	Elapsed Time, Max Distance Method	Elapsed Time, Threshold Method
1	MD231 (20Hz)	1726453	481.25 seconds	1.59 seconds
2	MD206 (20Hz)	1725882	397.93 seconds	1.25 seconds
3	MD202 (10Hz)	863046	314.10 seconds	0.65 seconds
4	MD226 (10Hz)	861678	145.13 seconds	1.11 seconds
5	MD259 (10Hz)	862690	162.74 seconds	0.67 seconds

As can be seen in Table 7.2, the time required to process the maximum distance method is much higher than the threshold method; in addition, this time is roughly double for data recorded with 20 Hz sampling rate. Therefore, based on the large observed processing time of the maximum

distance method, for the big data processing in Chapter 8 we will revert to the use of the simpler threshold method, and sometimes combine it with other indictors (e.g. SNR estimator) to determine the segments of data which should be kept for processing.

Chapter 8. Long-Term Monitoring

In this longitudinal sleep monitoring study, bed occupancy detection and breathing rate variabilities are the two main features that can be obtained. To decrease the computational complexity but also mostly to discard irrelevant data from the big data, occupancy detection is necessary. Therefore, the time-efficient threshold-based occupancy monitoring method presented in Chapter 7 was used on the big data to remove those data recorded during non-occupied times. This was done to keep only data related to the period of times that someone occupies the bed and discard the rest of data. By performing occupancy detection, some other relevant information can be captured such as the number of bed entries/exits and also the total amount of time a person spends in the bed, which were studied in this chapter.

In this chapter, after minimizing the processing complexity and discarding invalid data by keeping bed-occupied periods of recordings, the evolution of the breathing rate was investigated. For finding the breathing rate, first the breathing signal had to be determined. The method presented in Chapter 6 referred as SNR-max method [3] was used in order to extract the breathing signal. As movement artifacts were present in the breathing signal, movement detection was conducted to exclude breathing rate estimates associated with the artifacts. Since all bed-occupied times did not necessarily refer to times where respiratory information was available, identifying segments with strong breathing information was also required. These two steps needed to be performed prior to finding the final breathing rate variabilities of the big data. The scheme is described in detail in this chapter.

8.1. *Bed Occupancy Measurement*

The total time that a person spends in the bed regardless of his/her position (e.g. sitting, sleeping and moving) is considered as the occupancy duration. Therefore, the threshold-based occupancy detection method introduced in Chapter 7 can be efficiently applied on the big data in order to identify bed occupancy. Furthermore, the number of daily bed exits was determined from the occupancy indicator signal. This information could potentially be beneficial in terms of sleep quality analysis, however it also includes bed exits during non-sleep times. This could be improved by using the more complex but more accurate max distance based bed-occupancy method presented in Chapter 7.

Below you can see the results of bed occupancy and number of bed exits analysis for 9 participants described in Section 4.3 over the days for which their recording data was available. The typical results for bed occupancy and bed exits are shown in Figure 8.1 for Participant MD116. The results for the other eight participants are presented in Appendix A for further information. In Figure 8.1 (a), the occupancy duration, non-occupancy duration as well as the total time of recording are plotted over time on a daily-basis.

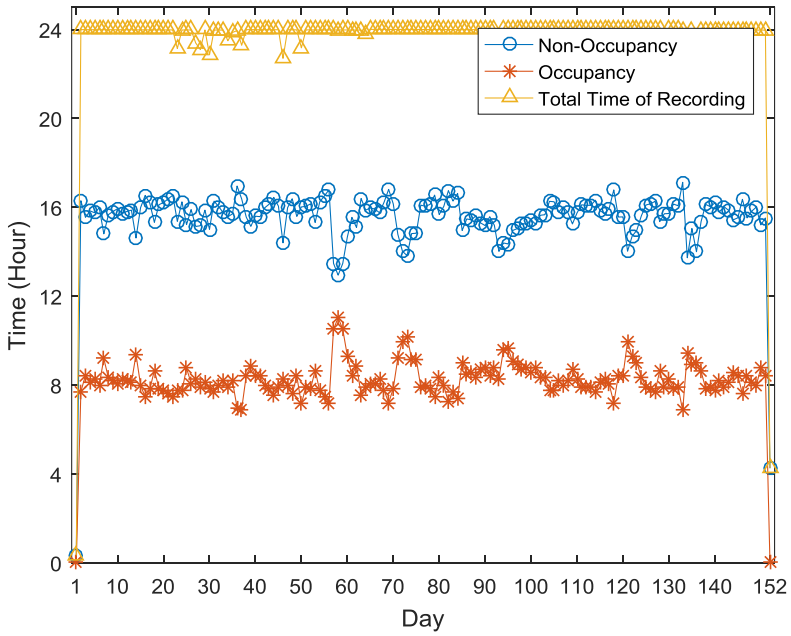

a) Bed Occupancy Analysis

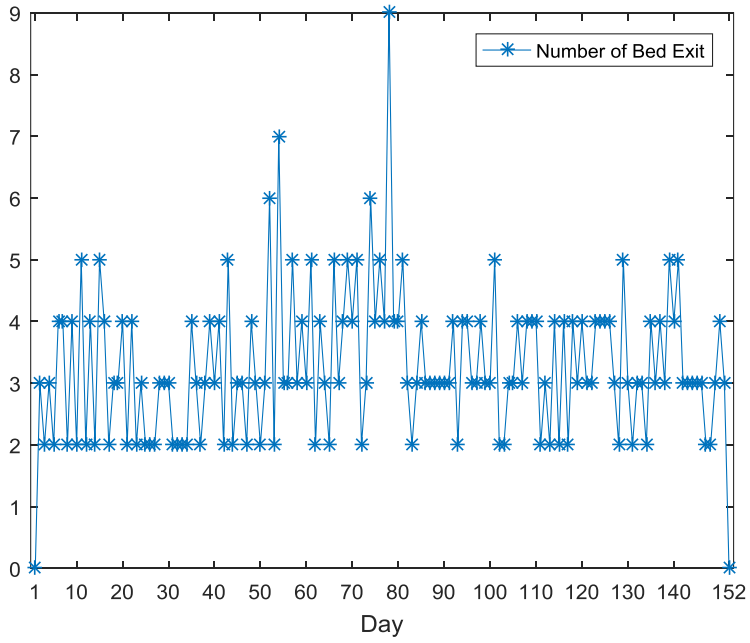

b) Number of Bed Exits per day

Figure 8.1. Bed occupancy analysis and number of bed exits per day for Patient MD116

As can be seen there are some days where recording was performed during slightly less than 24 hours. Probably, at some point the investigator may have needed to check the measurement set up so he/she had to stop the recording from time to time. Moreover, over reading the .csv files, some corrupted files were found and removed from the database. The data shortages in the recordings might be related to these two issues.

In the first and last day of recording for Participant MD116 no occupancy was captured in the data, and recordings much shorter than 24 hours were made. These days likely correspond to the days where the mat and the recording system were installed in the bedroom, and for which there was no one occupying the bedroom (e.g. no patient in the residence room).

8.2. *Breathing Rate Measurement*

As mentioned in Chapter 6 the SNR-max method overall outperformed other signal fusion methods for the extraction of breathing signal in data free of movement. Therefore, we used this method in order to measure the respiratory rate, but movements were required to be detected prior to rate estimation.

Our movement detection algorithm from Chapter 5 was computationally very heavy for big data processing and it was also configured based on a person's anthropometric information, which was not available for the people who participated in the big data collection project. Moreover, since there are large number of breathing rate estimates available in the big data, it is acceptable to discard samples of breathing rate estimates which occur during movement, as the remaining number of samples is still large. Therefore, a fast simple movement detection was used to flag movement segments and keep them away from further inclusion in longitudinal breathing rate measurements. This can easily be realized using the information related to the amplitude of the breathing signal; as mentioned in Chapter 5, movements cause high jumps in the breathing signal,

which are much bigger than any kind of breathing pattern (e.g. shallow breathing or deep breathing). The method used to discern movement segments is described as follows.

After band-pass filtering and segmentation of raw sensor array data as described in Chapter 5 and Chapter 6, the SNR-max signal fusion method was applied to get the respiratory signal. The breathing rate was then estimated from the respiratory signal in each segment by the auto-correlation method as mentioned in Chapter 6. The estimates which resulted from movement segments were then distinguished and put aside from further processing. To find movement segments, we used a method based on sub-segments absolute values. To do so, each segment was divided into five sub-segments. Then the maximum absolute value was obtained in each sub-segment. The number of sub-segments was selected in a way to avoid focusing on a local zero-crossing region in the segment signal, i.e., making sure that each sub-segment was long enough. Afterwards, a ratio was calculated for each segment based on dividing the higher maximum absolute level by the lower maximum absolute level from the five sub-segments. This ratio was used for classification of movement segments versus non-movement segments.

Based on our observation, in breathing segments most of the ratios were in the range of 2.2 to 3.8. Therefore, the threshold value chosen in this step discards only those segments with ratios higher than this threshold, without losing a large proportion of the data.

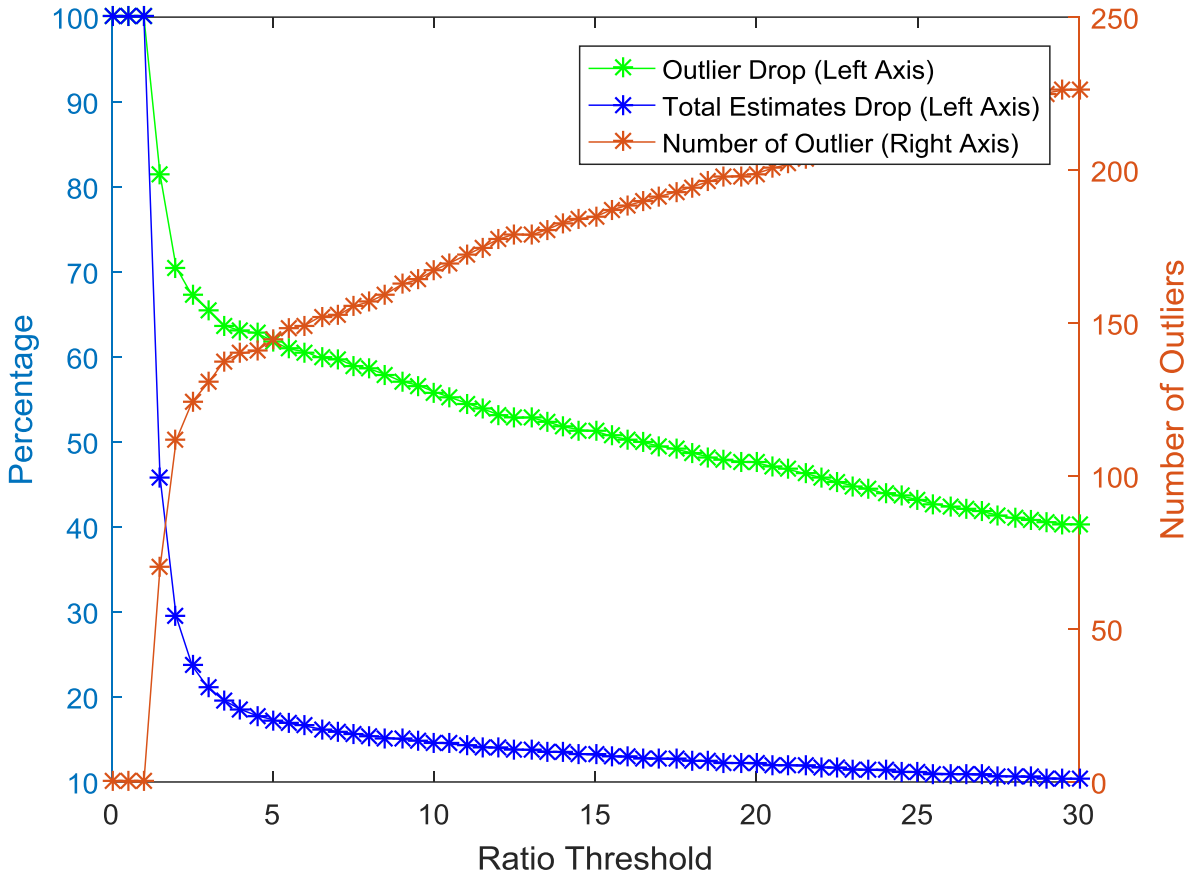

Figure 8.2. Effect of sub-segment ratio threshold on the number of outliers in breathing rate (BR) estimates, drop percentages in number of BR estimates and number of outliers

Figure 8.2 shows the effect of this ratio threshold on the percentage of removed segment estimates (blue curve), the total number of removed outliers in boxplots of the estimated BR (green curve), and the total number of remaining outliers in boxplots of the estimated BR (orange curve), for Participant MD116. The values shown in this figure are averaged over all days of recordings. Outliers are defined here in terms of boxplots as in Figure 8.4. Boxplots show a box representing the 25th and 75th percentiles of the data points as a box, and lines extending on both sides of the box are called the "whiskers". The length of the whiskers on both sides is 1.5 times the distance between the 25th and 75th percentiles (box length). The data points located outside of the whiskers

are then considered as outliers. As can be seen in Figure 8.2, there is a trade-off between the number of outliers and number of removed estimates relative to this threshold.

As discussed in Chapter 6, the max-distance bed-occupancy detection method can be computationally heavy. Therefore, for recognizing segments with low or no breathing information, the use of a simpler bed-occupancy detection method combined with additional SNR information was selected. The SNR was calculated for each segment by using spectral parameters (i.e., signal power and noise power in breathing rate frequency range), which were estimated based on the method described by Holtzman in [41]. According to this method, the power spectral density (PSD) is constructed from band-pass filtered segments. A modified periodogram is used to estimate the PSD, with Hanning windowed segments zero padded to a higher length which is power of two. It is assumed that in segments with available respiratory information, the highest peak corresponds to the fundamental frequency in the respiration band of interest (0.07 Hz to 0.8 Hz). Then, the main signal lobe is considered as the 3 dB width centered at the fundamental frequency. The median value of bins located in the respiratory band of interest but outside the main signal lobe and its probable harmonics, is the noise spectral density N_0. To estimate the total noise power N, the noise spectral density is integrated across the frequency band of interest, and the signal power S is estimated by integrating the power densities of the main signal lobe, with subtraction of the estimated noise power existing in the main signal lobe. Therefore, the SNR is calculated as:

$$SNR = \frac{S}{N} \tag{8.1}$$

We aimed to find a threshold for SNR to discard estimates which resulted from segments with low breathing signal power (with SNR below the chosen threshold). To do so, the percentage of

removed outliers was calculated for various SNR thresholds for each person over time. Then, the values were all averaged over the recording days. Typical results used to determine the SNR threshold are shown in Figure 8.3 for Participant MD116. The range of SNR threshold depicted in this figure is defined from the highest value of the daily minimum SNRs to the lowest value of the daily maximum SNRs.

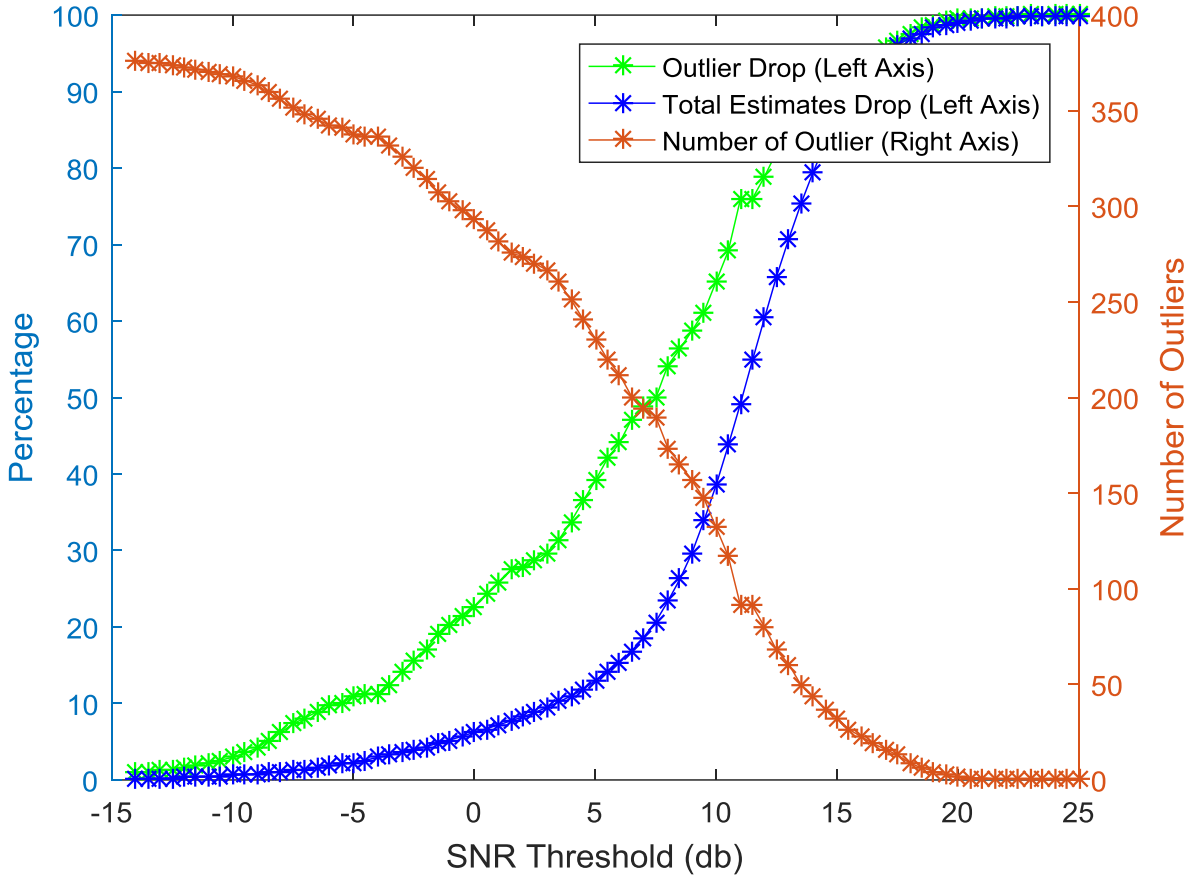

Figure 8.3. The effect of various SNR thresholds on the drop in the number of outliers in BR estimates, the drop percentage in the total number of BR estimates, and the number of remaining outliers in BR estimates

This approach was taken for all participants to avoid using of a constant SNR and ratio threshold, as different people with different size and breathing behaviors produced different SNR and ratio ranges.

After applying these two thresholds, the breathing rate variability and longitudinal analysis was obtained for each person with recordings available from the big data by depicting a boxplot as shown in Figure 8.4 (a) for Participant MD116. Moreover, the total time of the remaining segments kept for breathing rate estimation is shown versus the total time of the removed segments in Figure 8.4 (b) for Participant MD116. The results for the other eight participants are provided in Appendix B for further information.

The ratio threshold and SNR threshold chosen for Participant MD116 were 3 and 5, respectively. Each box in the boxplots is obtained from the segments kept for respiratory rate estimations after applying the two thresholds. The blank spaces in the boxplots refer to the days where no occupancy was captured (first and last day for Participant MD116).

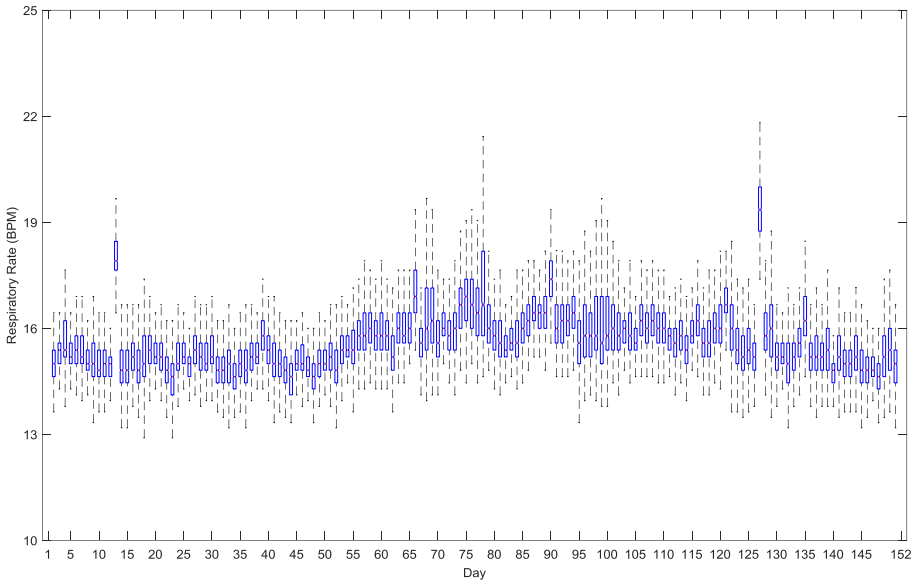

a) Boxplot of breathing rate variabilities over days

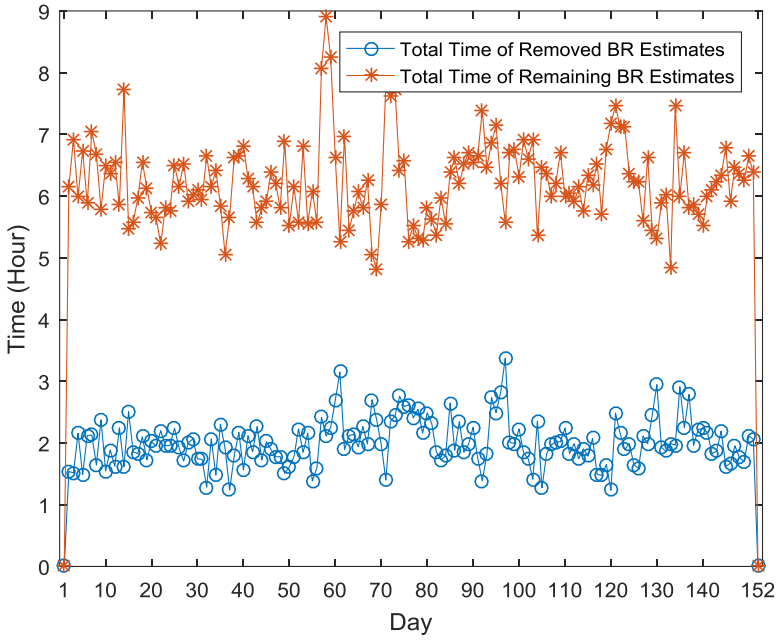

b) Total time of segments kept for breathing rate estimation vs. total time of removed segments

Figure 8.4. Breathing rate variability analysis and longitudinal study

8.3. *Concluding Remarks*

In this chapter, bed occupancy and breathing rate variability were investigated in a longitudinal study. The main purpose of pursuing this chapter was to observe older adults' sleep behavior over time, which is definitely a valuable measure from a clinical perspective. Knowing the rest of a person's medical record, some particular characteristics could possibly be identified from the extracted data, which might be associated to certain health conditions of the person.

Chapter 9. Conclusions and Future Work

In this thesis, we presented the culmination of our efforts towards physiological characteristics extraction from pressure sensitive sensors. The overall objective is to increase the level of wellbeing for users of such systems. First, we presented a real-time movement detection algorithm to prevent false breathing rate measurements during movement. Then we investigated the topic of signal combining to enhance quality of the breathing signal extracted from pressure mats, and we designed the SNR-max beam-forming method for signal combining. Bed-occupancy measurement methods were also presented from two perspectives: finding occupied times and finding occupied times with available sleep respiratory information. Both perspectives strive to achieve the same goal, although using different means. Since our work aims to be applicable for real-time use or offline use for big data analysis, we have applied the simpler version of these two algorithms on long-term data to observe variability of breathing rates and bed occupancy (or bed exits) over time. The objective is to achieve valuable results which might be useful for clinicians.

In order to perform the long-term sleep assessment described in this thesis, two main problems had to be solved. The first involves the discernment of movement segments and the second pertains to discard segments with low breathing signal information. Afterwards, breathing rate estimation on the remaining segments can reliably show each person's breathing behavior over time.

Some potential future work involves the implementation of the methods developed in this thesis as part of some monitoring or alarm system to detect sleep parameters in an online real-time fashion, since it could potentially allow saving lives. This would also be useful to improve the quality of present sleep characteristics detection applications.

Moreover, other feature extraction algorithms can be performed on the available big data set to attempt sleep-related disease detection (e.g. different types of apneas, etc.) and prediction of certain outcomes related to the possibility of certain illnesses in patients. In general, a lot of important information can be provided by big data analysis in the area of healthcare organization and in the healthcare industry.

References

[1] M. H. Jones, R. Goubran and F. Knoefel, "Identifying Movement Onset Times for a Bed-Based Pressure Sensor Array," *IEEE International Workshop on Medical Measurement and Applications, 2006. MeMea 2006.,* pp. 111-114, 2006.

[2] S. S. Gilakjani, S. Bennett, R. A. Goubran, H. Azimi, M. Bouchard and F. Knoefel, "Movement Detection with Adaptive Window Length for Unobtrusive Bed-Based Pressure-Sensor Array," *2017 IEEE International Symposium on Medical Measurements and Applications (MeMeA),* pp. 355-360, 2017.

[3] H. Azimi, S. S. Gilakjani, M. Bouchard, S. Bennett, R. A. Goubran and F. Knoefel, "Breathing Signal Combining for Respiration Rate Estimation in Smart Beds," *2017 IEEE International Symposium on Medical Measurements and Applications (MeMeA),* pp. 303-307, 2017.

[4] S. Soleimani, M. Bouchard, R. Goubran, H. Azimi and F. Knoefel, "Improved Sensor Selection Method during Movement for Breathing Rate Estimation with Unobtrusive Pressure Sensor Arrays," accepted with minor revisions for *IEEE International Sensors Application Symposium (SAS 2018),* March 2018.

[5] S. Soleimani, M. Bouchard, R. Goubran, H. Azimi and F. Knoefel, "Respiratory Rate Estimation by Unobtrusive Pressure Sensor Array During Movement," *Students' Poster Day 2017, Medical Devices Innovation Institute (MDII) and NSERC CREATE "Biomedical Engineering Smartphone Training" (BEST),* September 2017.

[6] H. Azimi, S. Soleimani, M. Bouchard, R. Goubran and F. Knoefel, "Automatic Apnea-Hypopnea Events Detection Using an Alternative Sensor," accepted with minor revisions for *IEEE International Sensors Application Symposium (SAS 2018),* March 2018.

[7] A. Rechtschaffen and A. Kales, A Manual of Standardized Terminology, Techniques, and Scoring Systems for Sleep Stages of Human Subjects, Los Angeles, CA: Brain Inf, 1968.

[8] L. J. Epstein, D. Kristo, P. J. J. Strollo, N. Friedman, A. Malhotra, S. P. Patil, K. Ramar, R. Rogers, R. J. Schwab, E. M. Weaver and M. D. Weinstein, "Clinical Guideline for the Evaluation, Management and Long-Term Care of Obstructive Sleep Apnea in Adults," *Journal of clinical sleep medicine : JCSM : official publication of the American Academy of Sleep Medicine,* vol. 5, no. 3, pp. 263-76, June 2009.

[9] P. Varady and S. Bongar, "Detection of Airway Obstruction and Sleep Apnea by Analyzing the Phase Relation of Respiration Movement Signals," *IMTC 2001. Proceedings of the 18th IEEE Instrumentation and Measurement Technology Conference. Rediscovering Measurement in the Age of Informatics (Cat. No. 01 CH 37188), Budapest,* vol. 1, pp. 185-190, 2001.

[10] G. Lavigne, P. Rompre and J. Montplaisir, "Sleep Bruxism: Validity of Clinical Research Diagnostic Criteria in a Controlled Polysomnographic Study," *Journal of Dental Research,* vol. 75, p. 546–552, 1996.

[11] C. Iber, S. Ancoli-Israel and A. Chesson, and Quan SF for the American Academy of Sleep Medicine, Terminology, T. Specifications and 1st, Eds., Illinois, : The AASM Manual for the Scoring of Sleep and Associated Events: Rules, 2007.

[12] N. A. Collop, S. L. Tracy, V. Kapur and others, "Obstructive Sleep Apnea Devices for Out-of-Center (OOC) Testing: Technology Evaluation," *Journal of Clinical Sleep Medicine,* vol. 7, p. 531–548, 2011.

[13] N. A. Collop, W. M. Anderson, B. Boehlecke and others, "Clinical Guidelines for the Use of Unattended Portable Monitors in the Diagnosis of Obstructive Sleep Apnea in Adult Patients," *Journal of Clinical Sleep Medicine,* vol. 3, p. 737–747, 2007.

[14] J. M. Kelly, R. E. Strecker and M. T. Bianchi, "Recent Developments in Home Sleep-Monitoring Devices," *ISRN Neurology,* vol. 2012, p. 10, 2012.

[15] R. Verrier, J. Hobson, E. Lovett and E. Pace-Schott, "Home-Based System and Method for Monitoring Sleep State and Assessing Cardiorespiratory Risk," *May 11 1999. US Patent 5,902,250.*

[16] K. L. Courtney, "Privacy and Senior Willingness to Adopt Smart Home Information Technology in Residential Care Facilities," *Methods of Information in Medicine,* vol. 47, no. 1, p. 76–81, 2008.

[17] Z. T. Beattie, C. C. Hagen, M. Pavel and T. L. Hayes, "Classification of Breathing Events Using Load Cells under the Bed, " *Conference Proceedings,* 2009, pp. 3921-3924.

[18] M. Brink, C. H. Muller and C. Schierz, "Contact-Free Measurement of Heart Rate, Respiration Rate, and Body Movements during Sleep," *Behav Res Methods,* 2006.

[19] G. S. Chung, B. H. Choi, D. U. Jeong and K. S. Park, "Noninvasive Heart Rate Variability Analysis Using Load-Cell Installed Bed during Sleep," *2007 29th Annual International Conference of the IEEE Engineering in Medicine and Biology Society,* pp. 2357-2360, 2007.

[20] A. M. Adami, M. Pavel, T. L. Hayes and C. M. Singer, "Detection of Movement in Bed Using Unobtrusive Load Cell Sensors," *in IEEE Transactions on Information Technology in Biomedicine,* vol. 14, pp. 481-490, March 2010.

[21] J. Alihanka, K. Vaahtoranta and I. Saarikivi, "A New Method for Long-Term Monitoring of the Ballistocardiogram, Heart Rate, and Respiration," *The American Journal of Physiology,* vol. 240, p. R384–92, May 1981.

[22] B. H. Jansen, B. H. Larson and K. Shankar, "Monitoring of the Ballistocardiogram with the Static Charge Sensitive Bed," *in IEEE Transactions on Biomedical Engineering,* vol. 38, pp. 748-751, August 1991.

[23] O. Polo, L. Brissaud, B. Sales, A. Besset and M. Billiard, "The Validity of the Static Charge Sensitive Bed in Detecting Obstructive Sleep Apneas," *European Respiratory Journal,* vol. 1, p. 330–336, 1988.

[24] E. Hoque, R. F. Dickerson and J. A. Stankovic, "Monitoring Body Positions and Movements during Sleep Using Wisps," in *Wireless Health 2010, ser*, WH '10. New York, NY, USA, ACM, 2010, pp. 44-53.

[25] A. Gaddam, S. C. Mukhopadhyay and G. S. Gupta, "Necessity of a Bed-Sensor in a Smart Digital Home to Care for Elder People," *2008 IEEE Sensors,* pp. 1340-1343, 2008.

[26] M. Holtzman, D. Townsend, R. Goubran and F. Knoefel, "Validation of Pressure Sensors for Physiological Monitoring in Home Environments," *2010 IEEE International Workshop on Medical Measurements and Applications,* pp. 38-42, 2010.

[27] D. Townsend, R. Goubran, F. Knoefel and J. Leech, "Validation of Unobtrusive Pressure Sensor Array for Central Sleep Apnea Screening," *in IEEE Transactions on Instrumentation and Measurement,* vol. 61, pp. 1857-1865, July 2012.

[28] D. Townsend, M. Holtzman, R. Goubran, M. Frize and F. Knoefel, "Relative Thresholding With Under-Mattress Pressure Sensors to Detect Central Apnea," *in IEEE Transactions on Instrumentation and Measurement,* vol. 60, pp. 3281-3289, October 2011.

[29] D. Townsend, R. Goubran and F. Knoefel, "Amplitude-Based Central Apnea Screening," *2011 IEEE International Symposium on Medical Measurements and Applications,* pp. 395-398, 2011.

[30] D. I. Townsend, M. Holtzman, R. Goubran, M. Frize and F. Knoefel, "Simulated Central Apnea Detection Using the Pressure Variance," *2009 Annual International Conference of the IEEE Engineering in Medicine and Biology Society,* pp. 3917-3920, 2009.

[31] M. Holtzman, A. Arcelus, R. Goubran and F. Knoefel, "Breathing Signal Fusion in Pressure Sensor Arrays," *2008 IEEE International Workshop on Medical Measurements and Applications,* pp. 71-76, 2008.

[32] M. H. Jones, R. Goubran and F. Knoefel, "Reliable Respiratory Rate Estimation from a Bed Pressure Array," *2006 International Conference of the IEEE Engineering in Medicine and Biology Society,* pp. 6410-6413, 2006.

[33] T. Harada, T. Sato and T. Mori, "Estimation of Bed-Ridden Human's Gross and Slight Movement based on Pressure Sensors Distribution Bed," in *Proc. IEEE Int. Conf. Robotics and Automation (ICRA)*, 2002.

[34] S. Poeggel, D. Tosi, D. Duraibabu, G. Leen, D. McGrath and E. Lewis, "Optical Fibre Pressure Sensors in Medical Applications, Basel, " *Switzerland:* Pavesi L, 2015.

[35] K. Sakai, G. Nakagami, N. Matsui, H. Sanada, A. Kitagawa, E. Tadaka and J. Sugama, "Validation and Determination of the Sensing Area of the Kinotex Sensor to Develop a New Mattress with an Interface Pressure-Sensing System," vol. 2, p. 36–43, 2008.

[36] E. M. Reimer and L. H. Baldwin, "Cavity Sensor Technology for Low Cost Automotive Safety and Control Devices," [Online]. Available: http://www.canpolar.com/principles.shtm. [Accessed 30 July 2006].

[37] M. Holtzman, A. Arcelus, I. Veledar, R. Goubran, H. Sveistrup and P. Guitard, "Force Estimation with a Non-Uniform Pressure Sensor Array," *2008 IEEE Instrumentation and Measurement Technology Conference,* pp. 1974-1979, 2008.

[38] D. Heise and M. Skubic, "Monitoring Pulse and Respiration with a Non-Invasive Hydraulic Bed Sensor," *2010 Annual International Conference of the IEEE Engineering in Medicine and Biology,* pp. 2119-2123, 2010.

[39] Y. Nishida, M. Takeda, T. Mori, H. Mizoguchi and T. Sato, "Monitoring Patient Respiration and Posture Using Human Symbiosis System, Intelligent Robots and Systems," *IROS '97., Proceedings of the 1997 IEEE/RSJ International Conference on, Grenoble,* vol. 2, pp. 632-639, September 1997.

[40] M. Holtzman, D. Townsend, R. Goubran and F. Knoefel, "Breathing Sensor Selection during Movement," *2011 Annual International Conference of the IEEE Engineering in Medicine and Biology Society,* pp. 381-384, 2011.

[41] M. Holtzman, "Robust Ambient Multisensor Signal Fusion towards Clinical Data Analytics, " PhD thesis, University of Carleton, Ottawa, ON, Canada, 2014.

[42] D. I. Townsend, M. Holtzman, R. Goubran, M. Frize and F. Knoefel, "Measurement of Torso Movement With Delay Mapping Using an Unobtrusive Pressure-Sensor Array," *in IEEE Transactions on Instrumentation and Measurement,* vol. 60, pp. 1751-1760, May 2011.

[43] D. Townsend, "Context-Aware Algorithms for Sleep Apnea Monitoring and Sensor Acceptance Using Unobtrusive Pressure Sensor Arrays," PhD thesis, University of Carleton, Ottawa, ON, Canada, 2012.

[44] M. Holtzman, R. Goubran and F. Knoefel, "Maximal Ratio Combining for Respiratory Effort Extraction from Pressure Sensor Arrays," *2011 IEEE International Symposium on Medical Measurements and Applications,* pp. 88-92, 2011.

[45] K. Nakajima, Y. Matsumoto and T. Tamura, "A Monitor for Posture Changes and Respiration in Bed Using Real Time Image Sequence Analysis," *in Proc. IEEE 22nd Ann. Int. Conf. Eng. Medicine Biology Society,* p. 51–54, 2000.

[46] M. Pouliot, V. Joshi, R. Goubran and F. Knoefel, "Bed Occupancy Monitoring: Data Processing and Clinician User Interface Design," *2012 Annual International Conference of the IEEE Engineering in Medicine and Biology Society,* 2012.

[47] J. -H. Kim, R. Roberge, J. B. Powell, a. B. Shafer and W. J. Williams, "Measurement Accuracy of Heart Rate and Respiratory Rate during Graded Exercise and Sustained Exercise in the Heat Using the Zephyr BioHarness," *Sports, Int. J.,* vol. 34, 2013.

[48] L. Tarassenko, M. Villarroel, A. Guazzi, J. Jorge, D. A. Clifton and C. Pugh, "Non-Contact video-Based Vital Sign Monitoring Using Ambient Light and Auto-Regressive Models," *Physiological Measurement,* vol. 35, 28 March 2014.

[49] M. H. Li, A. Yadollahi and B. Taati, "A Non-Contact Vision-Based System for Respiratory Rate Estimation," in *2014 36th Annual International Conference of the IEEE Engineering in Medicine and Biology Society*, Chicago, IL, 2014.

[50] V. Nguyen, A. Q. Javaid and M. A. Weitnauer, "Harmonic Path (HAPA) Algorithm for Non-Contact Vital Signs Monitoring with IR-UWB Radar," in *2013 IEEE Biomedical Circuits and Systems Conference (BioCAS)*, Rotterdam, 2013.

[51] J. J. Liu, M. C. Huang, W. Xu, X. Zhang, L. Stevens, N. Alshurafa and M. Sarrafzadeh, "BreathSens: A Continuous On-Bed Respiratory Monitoring System With Torso Localization Using an Unobtrusive Pressure Sensing Array," *IEEE Journal of Biomedical and Health Informatics,* vol. 19, pp. 1682-1688, September 2015.

[52] J. Werth, L. Atallah, P. Andriessen, X. Long, E. Zwartkruis-Pelgrim and R. Aarts, "Unobtrusive Sleep State Measurements in Preterm Infants - a Review," *Sleep Med.,* pp. 109-122, 2017.

[53] J. Benesty, J. Chen and Y. Huang, "Microphone Array Signal Processing," Springer Science & Business Media, 2008.

[54] D. Lo, R. A. Goubran, R. M. Dansereau, G. Thompson and D. Schulz, "Robust Joint Audio-Video Localization in Video Conferencing Using Reliability Information," *IEEE Trans. Instrumentation and Measurement,* vol. 53, p. 1132–1139, 2004.

[55] M. Bosi and R. E. Goldberg, "Introduction to Digital Audio Coding and Standards," 1 ed., Springer US, 2002.

[56] H. F. M. Van der Loos, N. Ullrich and H. Kobayashi, "Development of Sensate and Robotic Bed Technologies for Vital Signs Monitoring and Sleep Quality Improvement," *Autonomous Robots,* vol. 15, pp. 67-79, July 2003.

[57] C. L. Mason and L. Tarassenko, "Quantitative Assessment of Respiratory Derivation Algorithms," *2001 Conference Proceedings of the 23rd Annual International Conference of the IEEE Engineering in Medicine and Biology Society,* vol. 2, pp. 1998-2001, 2001.

Appendix A

The results of bed occupancy analysis and daily bed exit patterns for the other eight participants are presented in this section.

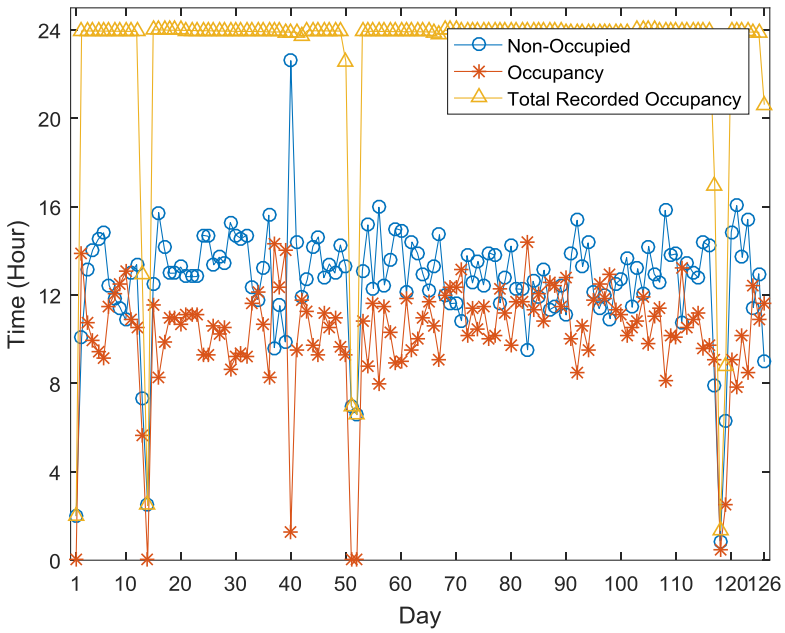

a) Bed Occupancy Analysis

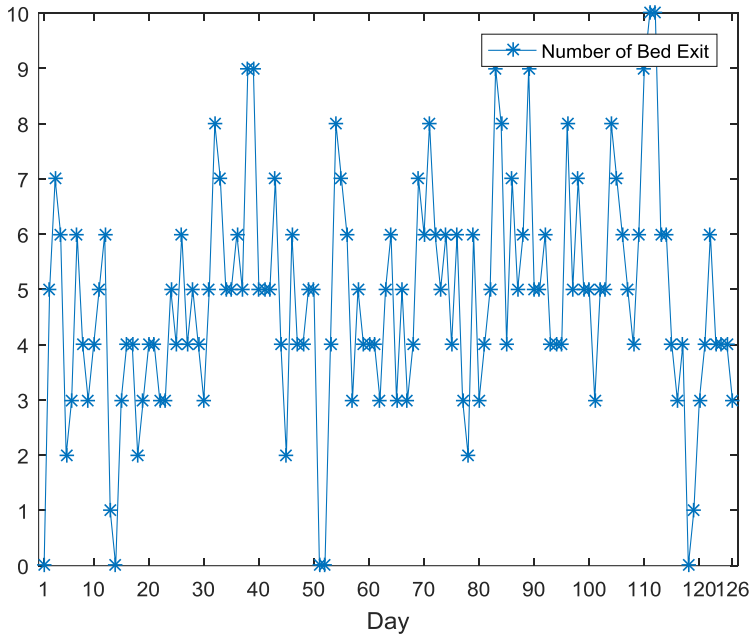

b) Number of Bed Exits per day

Figure A.1. Bed occupancy analysis and number of bed exits per day for Participant MD139

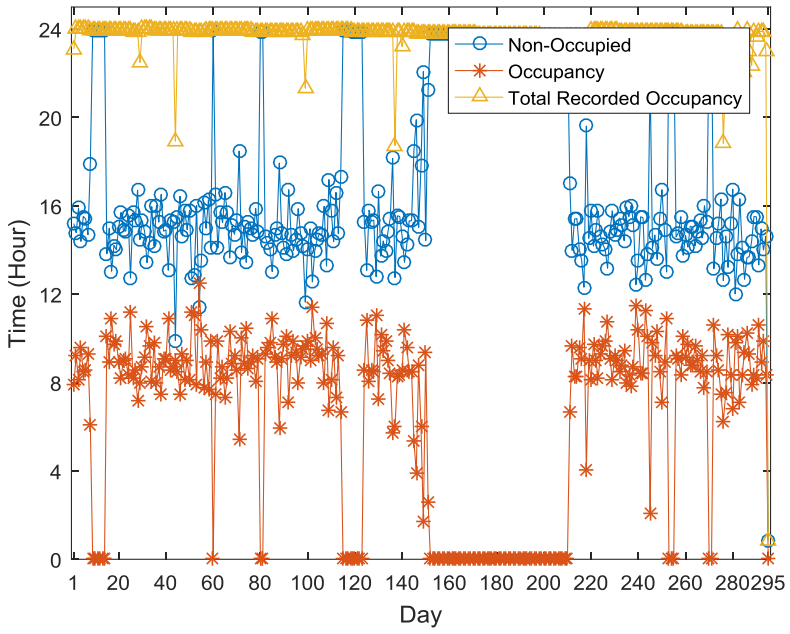

a) Bed Occupancy Analysis

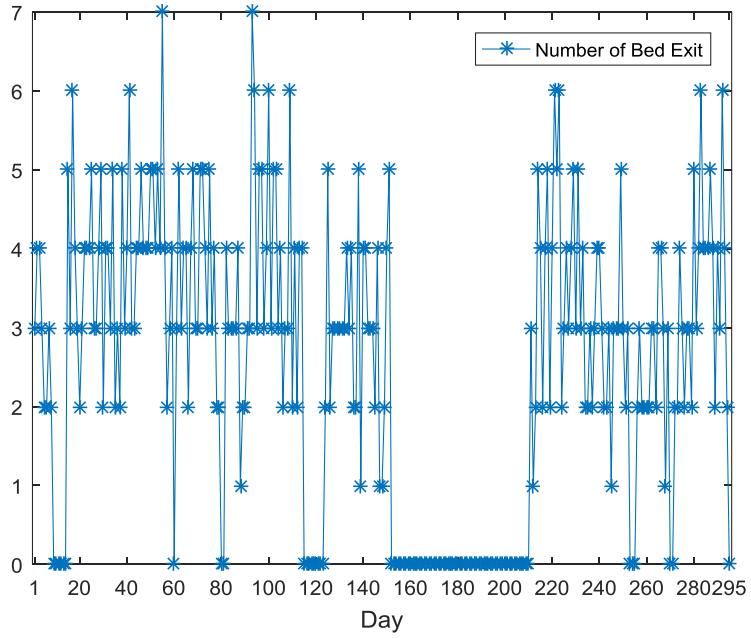

b) Number of Bed Exits per day

Figure A.2. Bed occupancy analysis and number of bed exits per day for Participant MD185

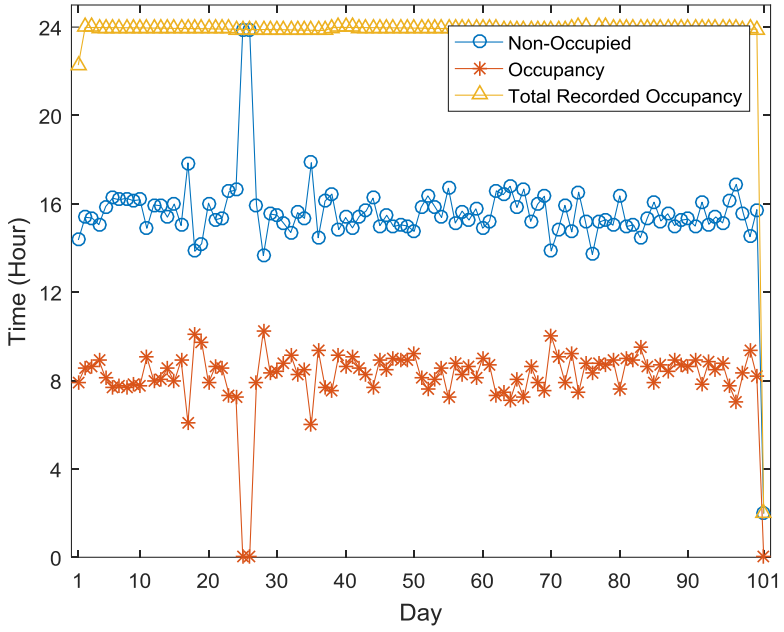

a) Bed Occupancy Analysis

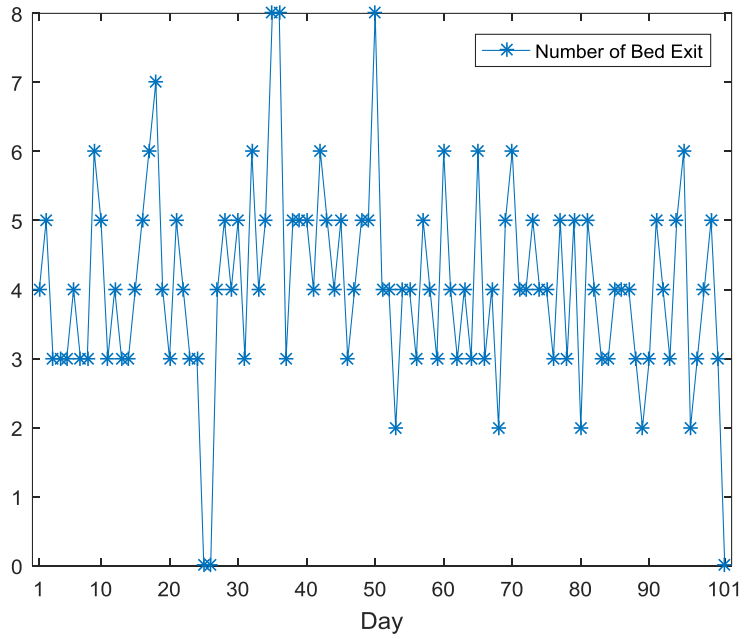

b) Number of Bed Exits per day

Figure A.3. Bed occupancy analysis and number of bed exits per day for Participant MD202

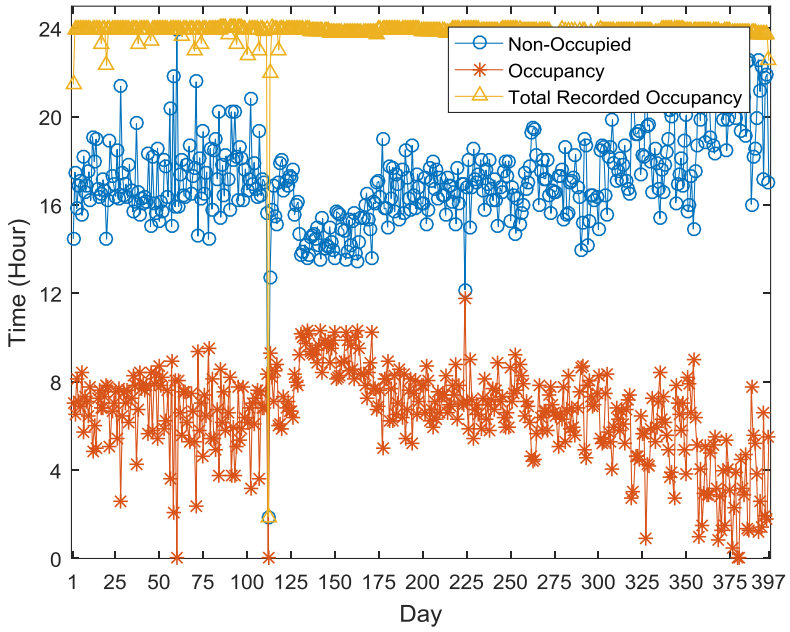

a) Bed Occupancy Analysis

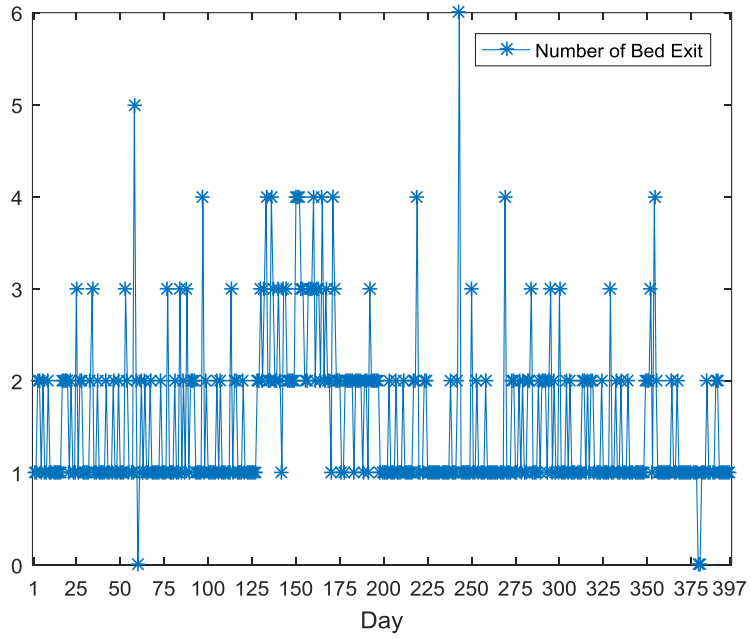

b) Number of Bed Exits per day

Figure A.4. Bed occupancy analysis and number of bed exits per day for Participant MD206

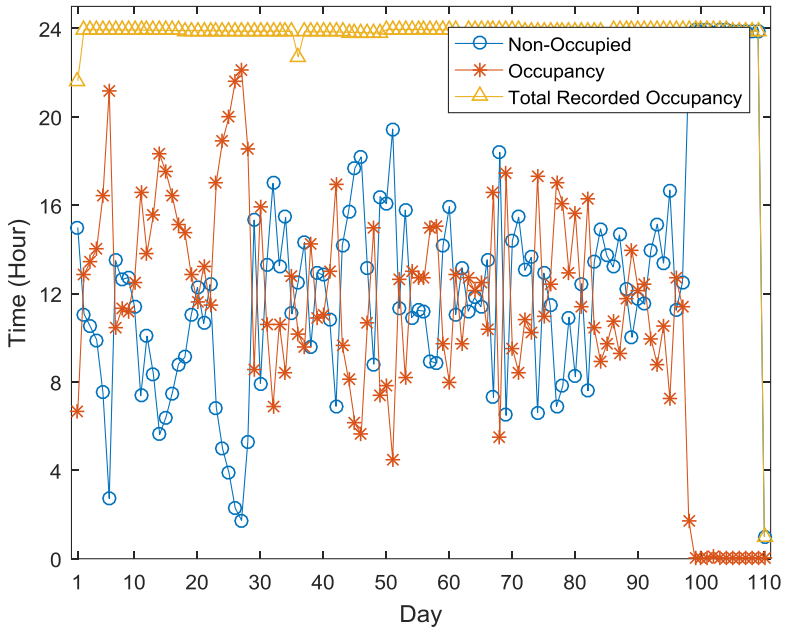

a) Bed Occupancy Analysis

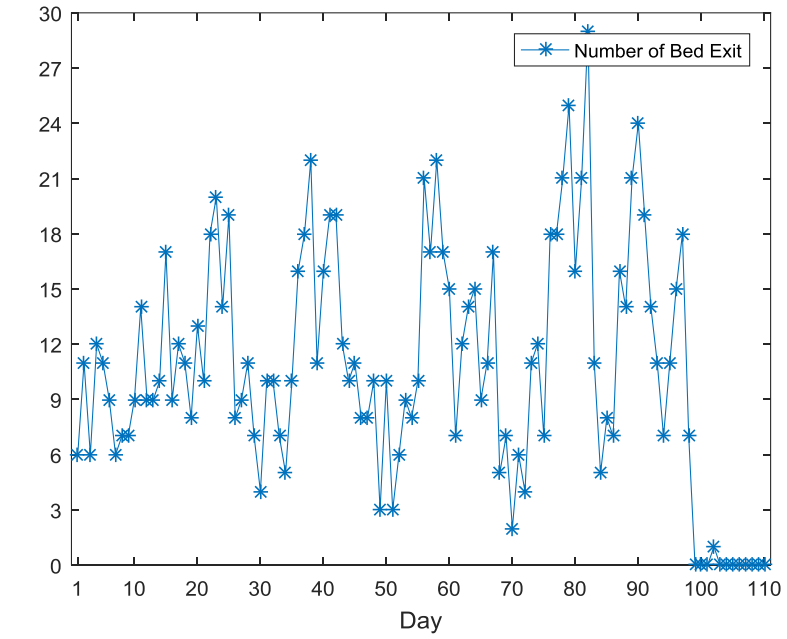

b) Number of Bed Exits per day

Figure A.5. Bed occupancy analysis and number of bed exits per day for Participant MD226

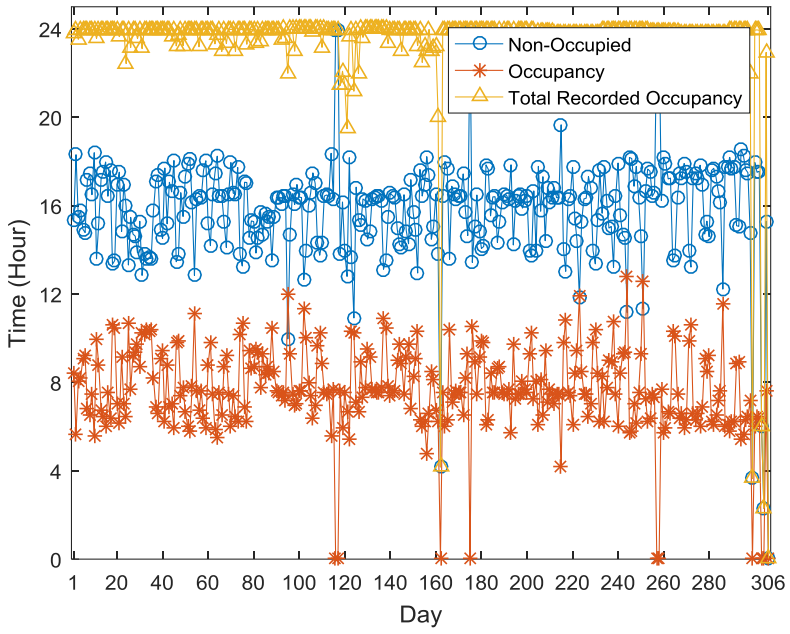

a) Bed Occupancy Analysis

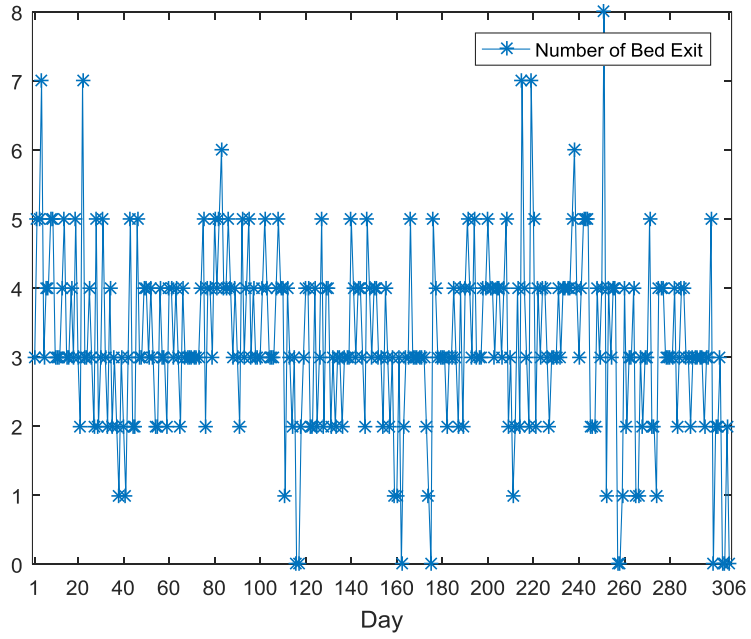

b) Number of Bed Exits per day

Figure A.6. Bed occupancy analysis and number of bed exits per day for Participant MD231

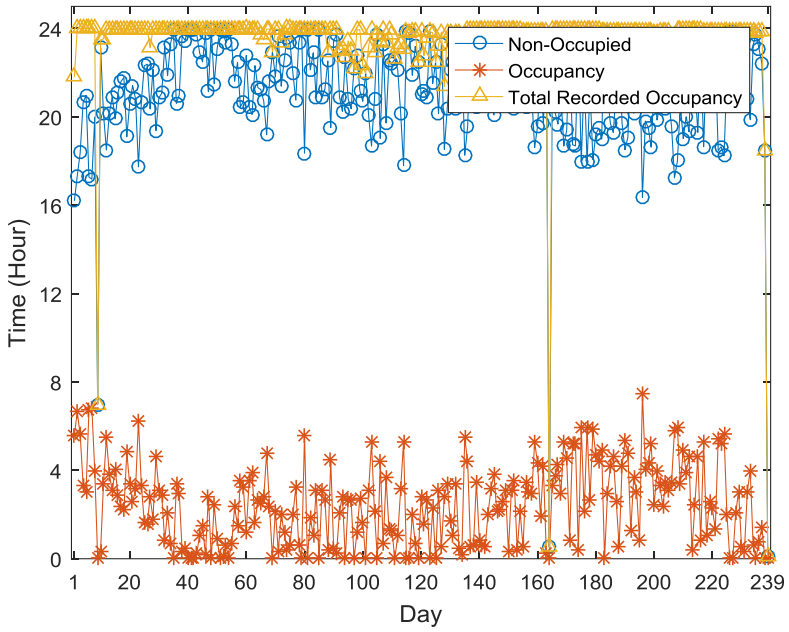

a) Bed Occupancy Analysis

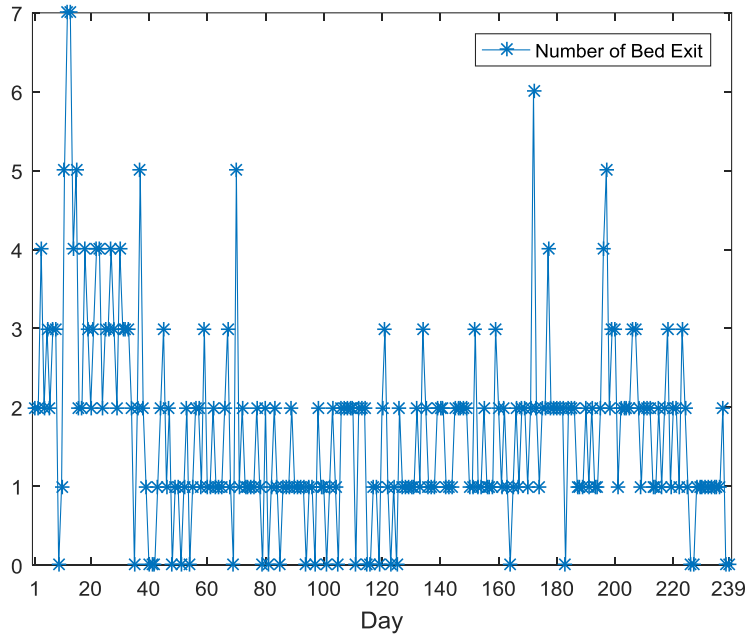

b) Number of Bed Exits per day

Figure A.7. Bed occupancy analysis and number of bed exits per day for Participant MD442

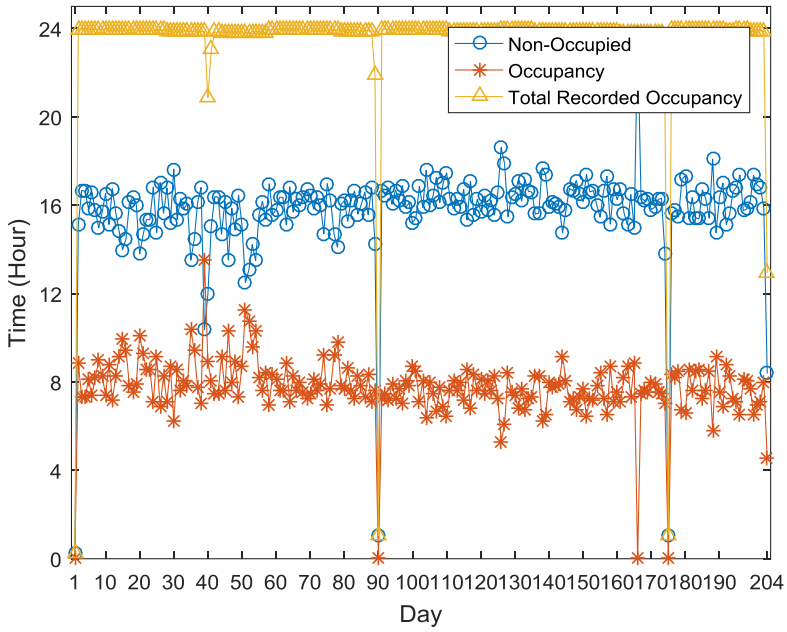

a) Bed Occupancy Analysis

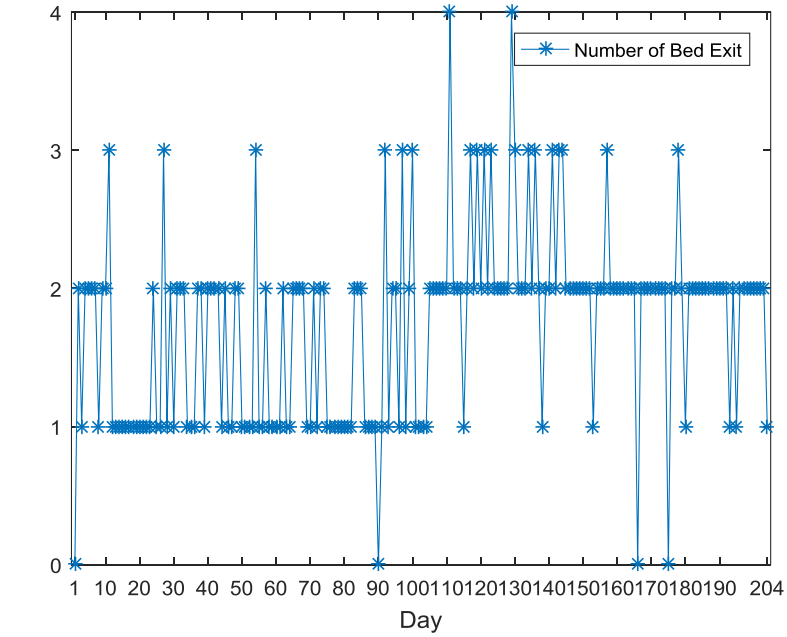

b) Number of Bed Exits per day

Figure A.8. Bed occupancy analysis and number of bed exits per day for Participant MD259

Appendix B

The results of breathing rate variabilities for the other eight participants are presented in this section.

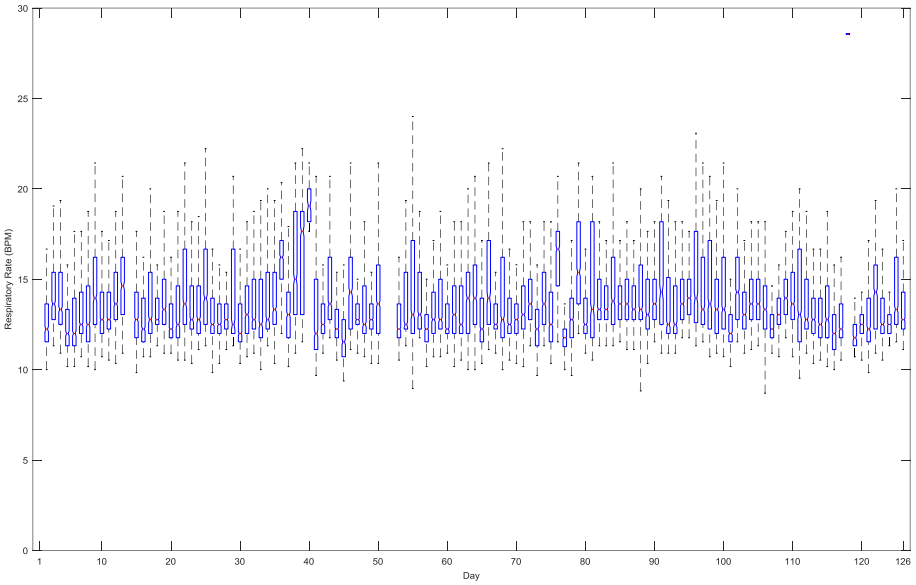

a) Boxplot of breathing rate variabilities over consecutive days

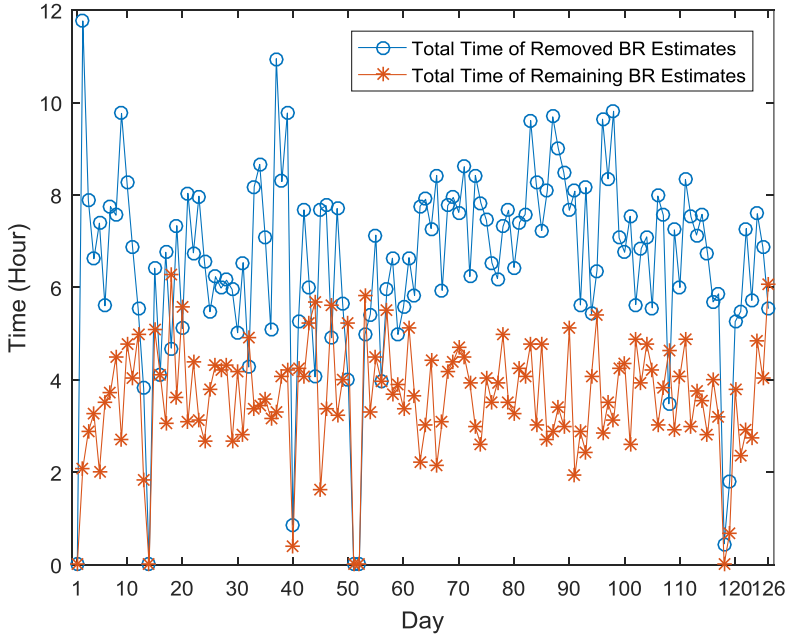

b) Total time of segments kept for breathing rate estimation vs. total time of removed segments

Figure B.1. Breathing rate variability analysis and longitudinal study for Participant MD139

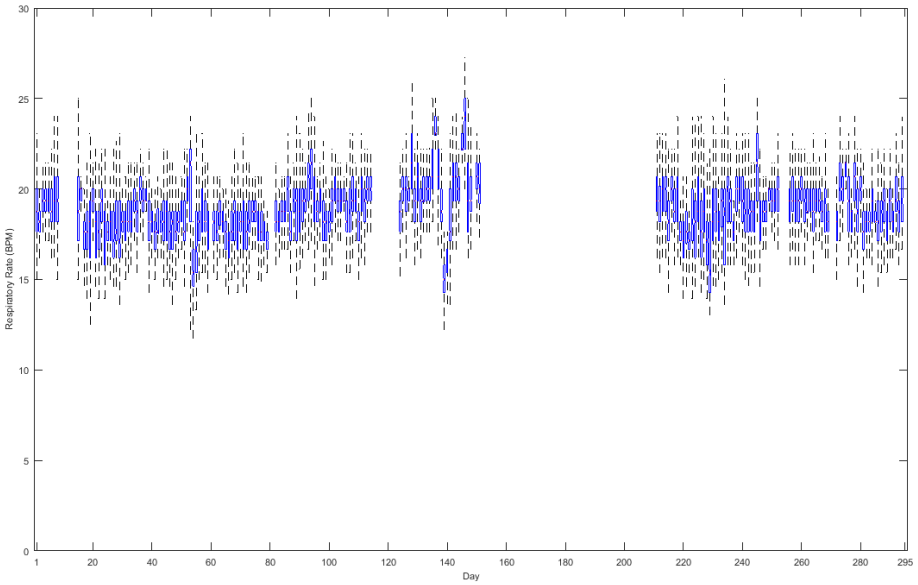

a) Boxplot of breathing rate variabilities over consecutive days

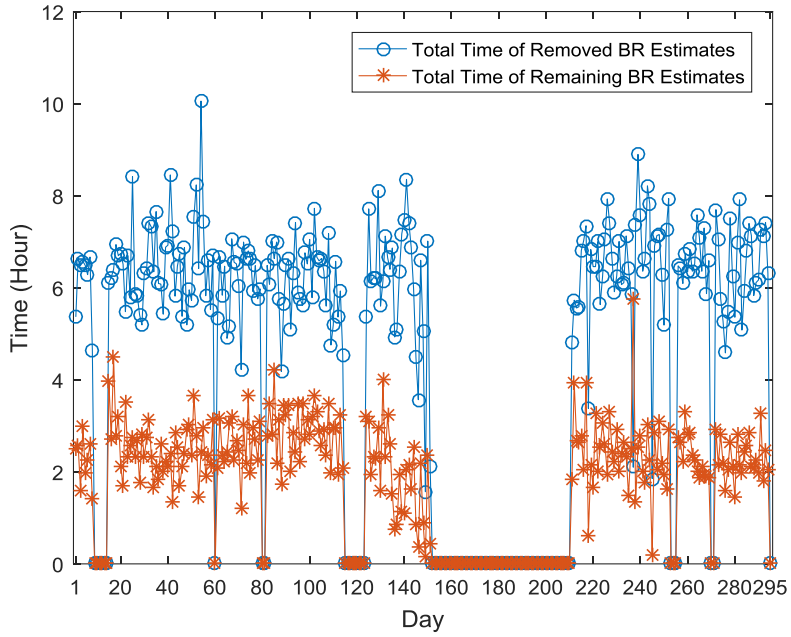

b) Total time of segments kept for breathing rate estimation vs. total time of removed segments

Figure B.2. Breathing rate variability analysis and longitudinal study for Participant MD185

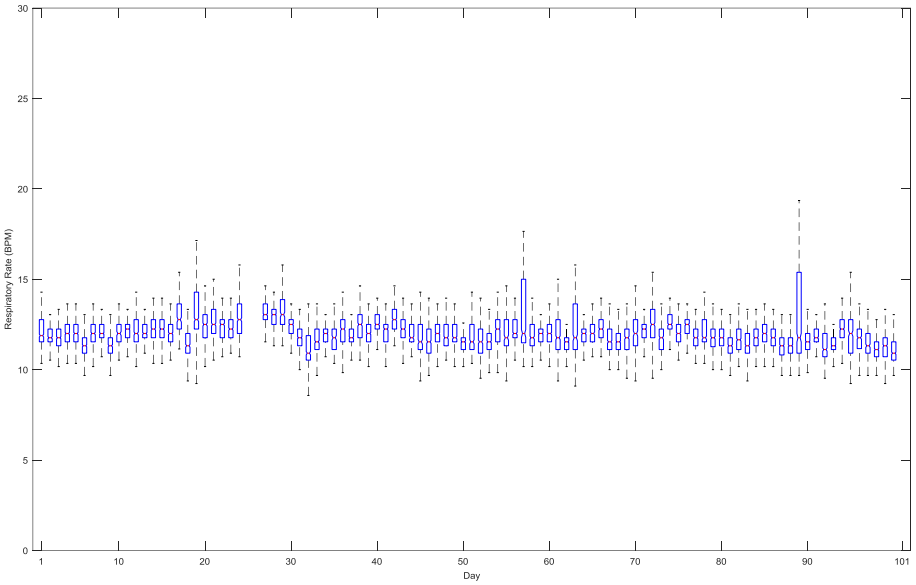

a) Boxplot of breathing rate variabilities over consecutive days

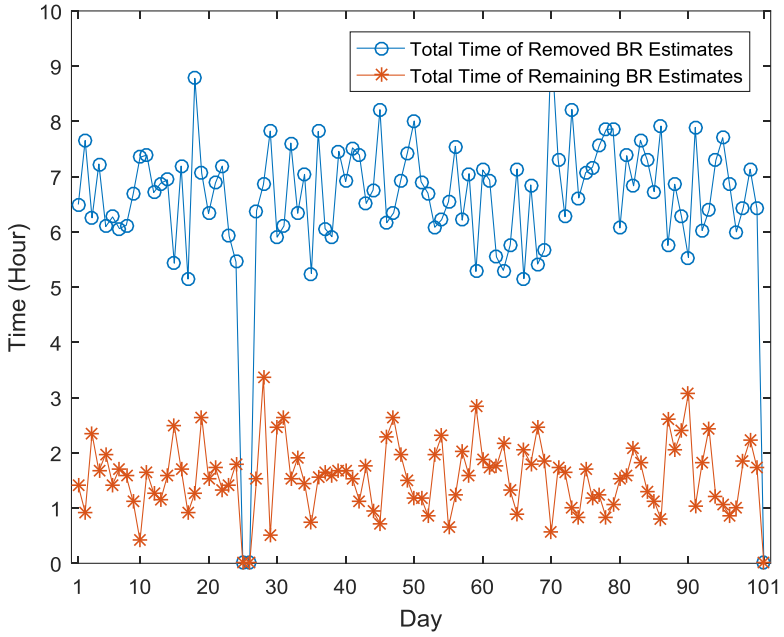

b) Total time of segments kept for breathing rate estimation vs. total time of removed segments

Figure B.3. Breathing rate variability analysis and longitudinal study for Participant MD202

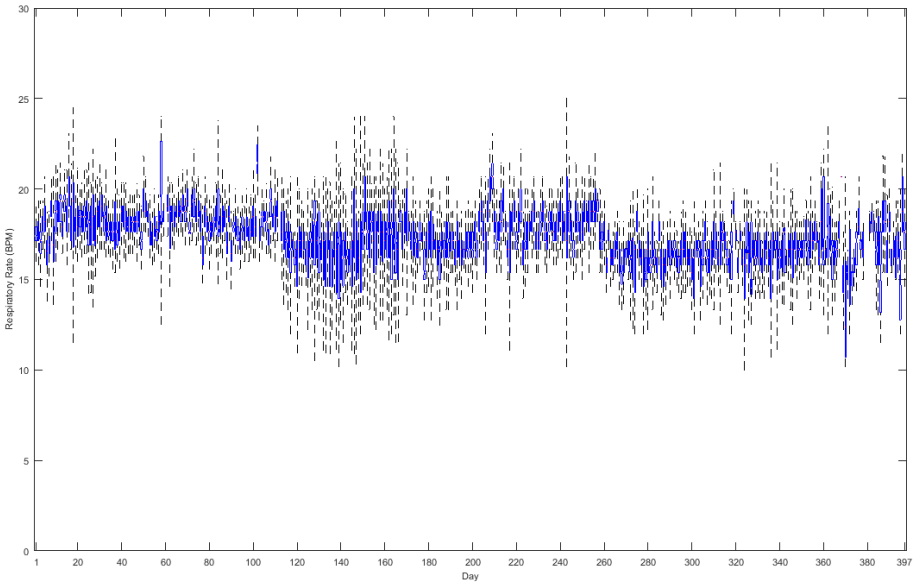

a) Boxplot of breathing rate variabilities over consecutive days

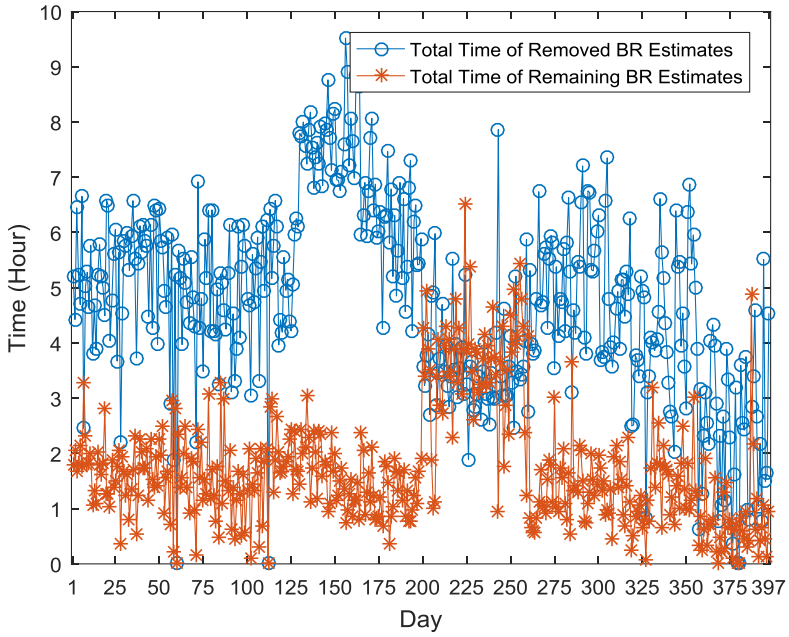

b) Total time of segments kept for breathing rate estimation vs. total time of removed segments

Figure B.4. Breathing rate variability analysis and longitudinal study for Participant MD206

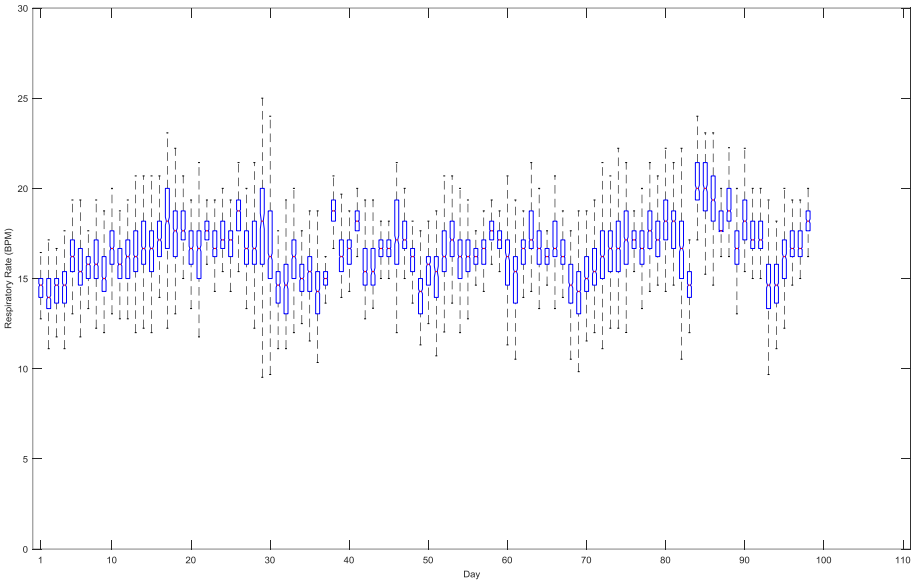

a) Boxplot of breathing rate variabilities over consecutive days

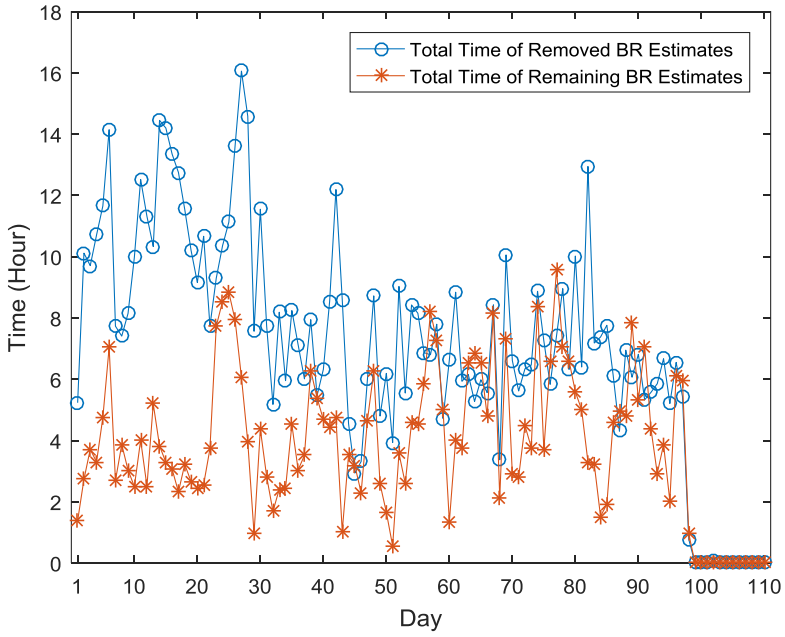

b) Total time of segments kept for breathing rate estimation vs. total time of removed segments

Figure B.5. Breathing rate variability analysis and longitudinal study for Participant MD226

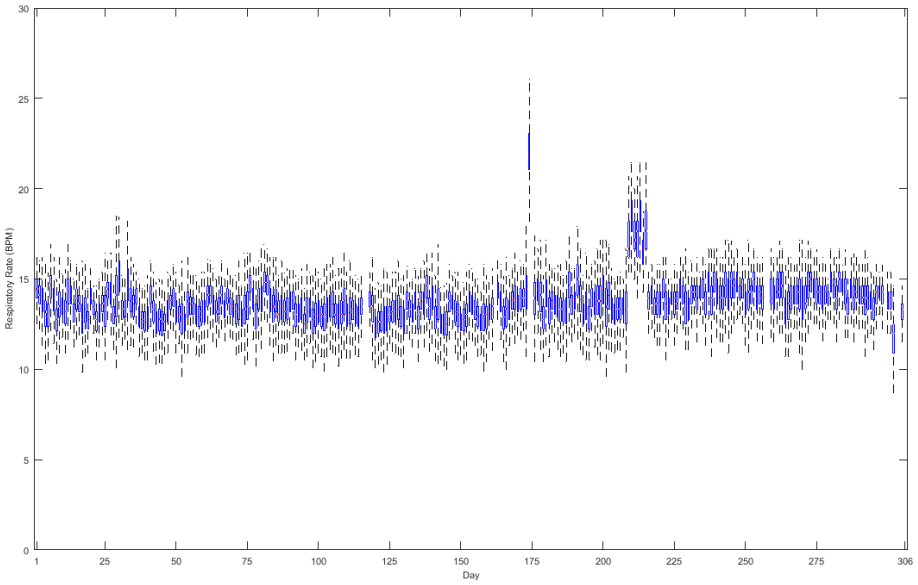

a) Boxplot of breathing rate variabilities over consecutive days

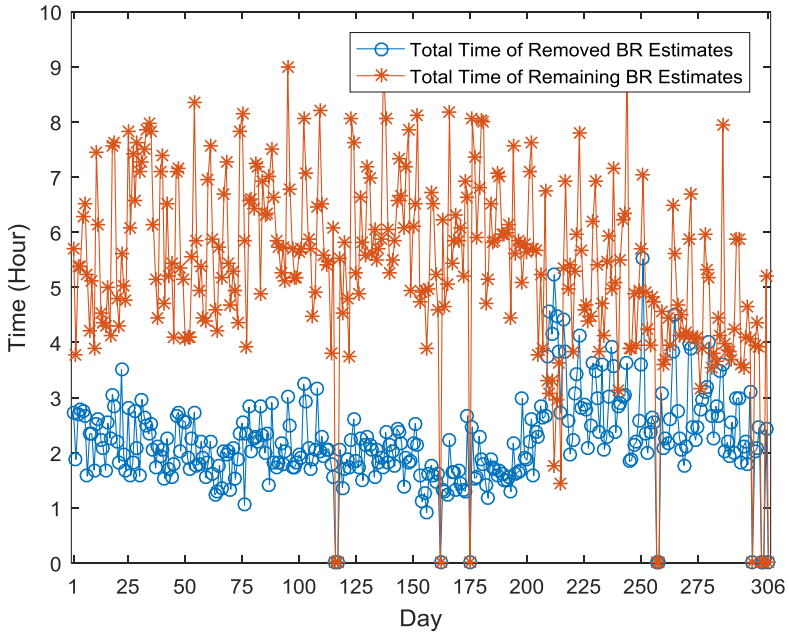

b) Total time of segments kept for breathing rate estimation vs. total time of removed segments

Figure B.6. Breathing rate variability analysis and longitudinal study for Participant MD231

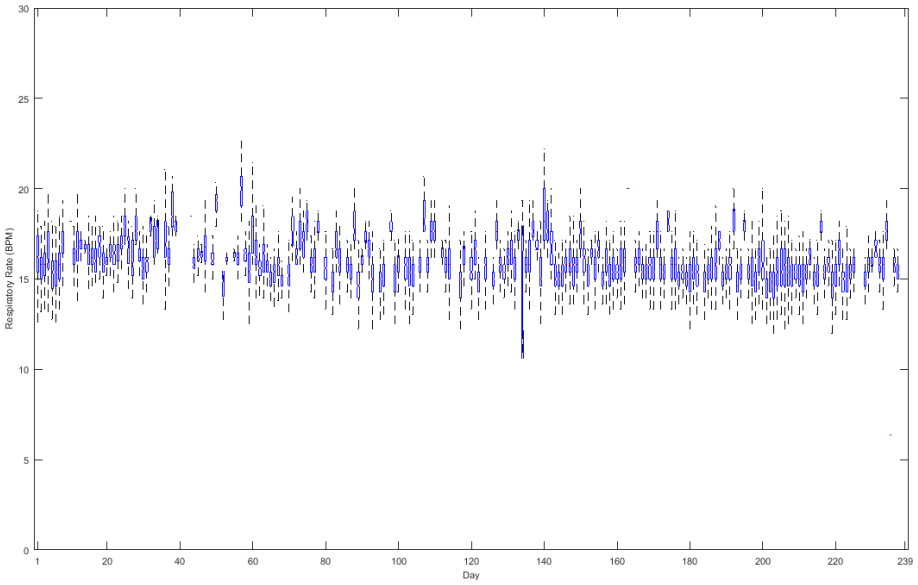

a) Boxplot of breathing rate variabilities over consecutive days

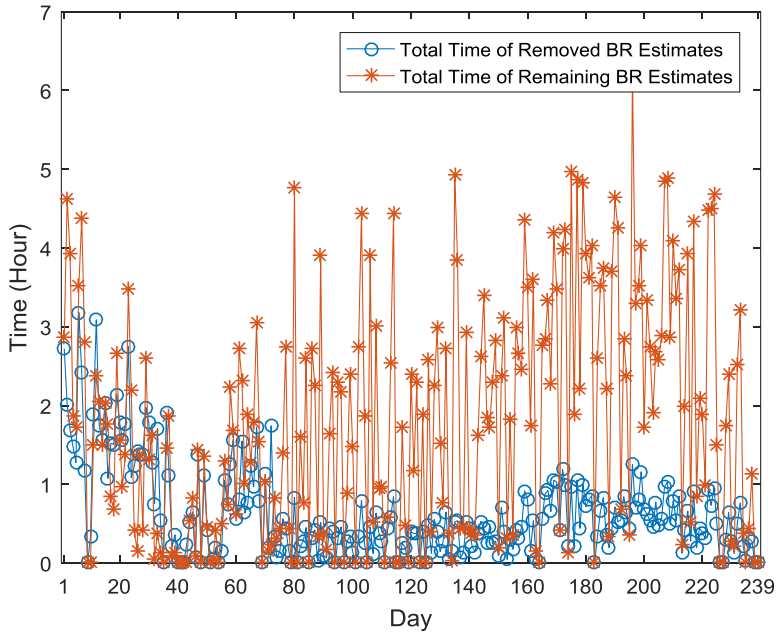

b) Total time of segments kept for breathing rate estimation vs. total time of removed segments

Figure B.7. Breathing rate variability analysis and longitudinal study for Participant MD442

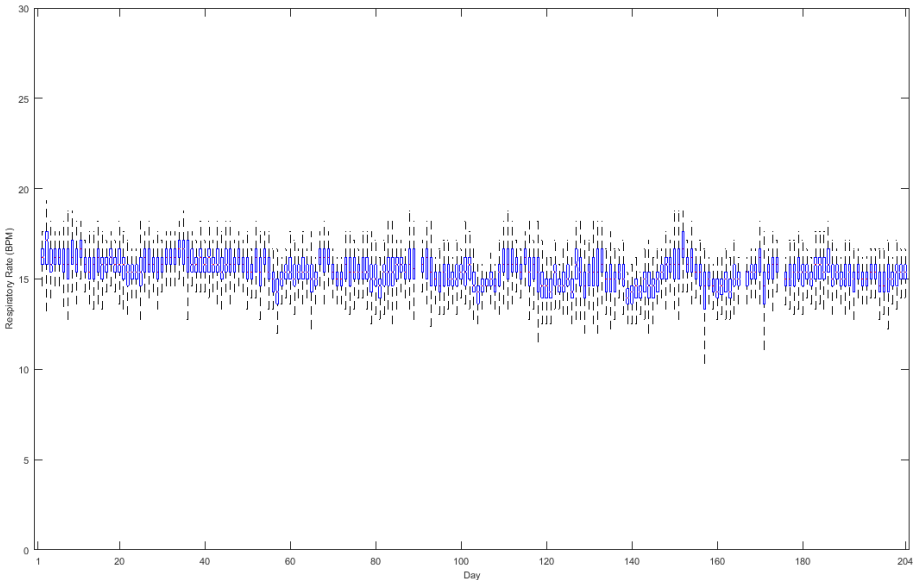

a) Boxplot of breathing rate variabilities over consecutive days

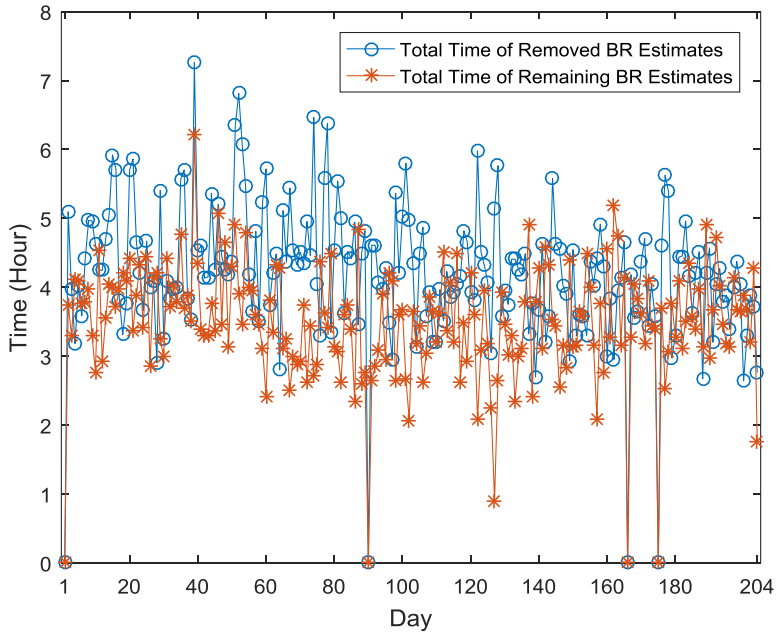

b) Total time of segments kept for breathing rate estimation vs. total time of removed segments

Figure B.8. Breathing rate variability analysis and longitudinal study for Participant MD259